



HAL
open science

Entropy Scaling-Based Correlation for Estimating the Self-Diffusion Coefficients of Pure Fluids

Aghilas Dehlouz, Jean-Noël Jaubert, Guillaume Galliero, Marc Bonnissel,
Romain Privat

► **To cite this version:**

Aghilas Dehlouz, Jean-Noël Jaubert, Guillaume Galliero, Marc Bonnissel, Romain Privat. Entropy Scaling-Based Correlation for Estimating the Self-Diffusion Coefficients of Pure Fluids. *Industrial and engineering chemistry research*, 2022, 61 (37), pp.14033 - 14050. 10.1021/acs.iecr.2c01086 . hal-03787047

HAL Id: hal-03787047

<https://hal.univ-lorraine.fr/hal-03787047>

Submitted on 23 Sep 2022

HAL is a multi-disciplinary open access archive for the deposit and dissemination of scientific research documents, whether they are published or not. The documents may come from teaching and research institutions in France or abroad, or from public or private research centers.

L'archive ouverte pluridisciplinaire **HAL**, est destinée au dépôt et à la diffusion de documents scientifiques de niveau recherche, publiés ou non, émanant des établissements d'enseignement et de recherche français ou étrangers, des laboratoires publics ou privés.



Distributed under a Creative Commons Attribution - NonCommercial - NoDerivatives 4.0 International License

Entropy Scaling-Based Correlation for Estimating the Self-Diffusion Coefficients of Pure Fluids

Aghilas Dehlouz, Jean-Noël Jaubert,* Guillaume Galliero, Marc Bonnissel, and Romain Privat*

 Cite This: *Ind. Eng. Chem. Res.* 2022, 61, 14033–14050

 Read Online

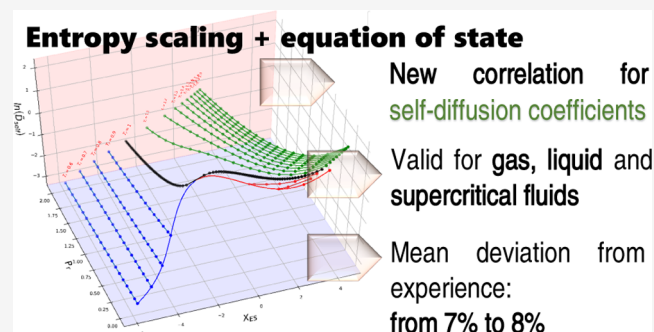
ACCESS |

 Metrics & More

 Article Recommendations

 Supporting Information

ABSTRACT: A new model for correlating self-diffusion coefficients is proposed here. It is based on the entropy scaling concept and makes it possible to quantitatively estimate self-diffusion coefficients in any fluid state (subcritical gas and liquid as well as supercritical states). A general relationship between a dimensionless form of the self-diffusion coefficient and a function of the Tv -residual entropy is proposed. This relationship involves thermodynamic properties that were straightforwardly estimated using the I -PC-SAFT and tc -PR equations of state (EoS). First, the proposed model was parameterized using component-specific parameters. To do so, 72 pure components and ~ 2400 pieces of experimental data were considered. Second, a chemical-family parametrization method was used. Four chemical families were defined, and parameter sets valid for all of the compounds of a given family were estimated. Regardless of the considered EoS, the component-specific parametrization enables us to describe data with an average deviation of 7.5%, while when using a chemical-family parametrization, this deviation reaches 9.5%.



INTRODUCTION

Transport phenomena characterize the situation where the flux density of a property α (amount of substance, momentum, heat) is generated by a driving force that is defined as the gradient of an intensive property f such as concentration or temperature. This force can thus be seen as a stimulus and the flux as the response to this stimulus.

All transport phenomena are characterized macroscopically by similar constitutive laws expressing a linear relationship between the flux density J (per unit of time and area) of the property α and the gradient ∇f of the associated intensive quantity f : $J_\alpha = -k\nabla f$. The proportionality constant k is called the transport coefficient and is a positive scalar.

If J_α is a diffusion flux density of which the dimension is the amount of substance (e.g., kg or mol) per unit area and per unit time (e.g., if the amount is a mass, the flux density is expressed in $\text{kg s}^{-1} \text{m}^{-2}$), then, f is the corresponding concentration (e.g., kg m^{-3}), $k = D$ is the mass diffusion coefficient ($\text{m}^2 \text{s}^{-1}$), and the corresponding constitutive law is known as Fick's law.

In the present article, the estimation of self-diffusion coefficients (denoted D_{self} hereafter)—a specific class of diffusion coefficients—is addressed.

In practice, self-diffusion coefficients are used to quantitatively describe various phenomena that are driven by molecular dynamics at the microscopic scale. For instance, self-diffusion is involved in the characterization of nanoporous material for gas production, storage and separation,^{1–3} and in the analysis of the protein hydration layer.⁴ It is used to correlate ionic transport behavior⁵ and the glass transition of nanoconfined polymers⁶ as

well as for expressing binary mass diffusion coefficients D_{ij} .^{7–10} It is also widely used to quantify the migration of tracers in various contexts^{11,12} as the mass diffusion of a tracer is fully defined by its self-diffusion coefficient. Various experimental techniques,¹³ such as the tracer method, nuclear magnetic resonance, or neutron scattering method, can be implemented to measure self-diffusion coefficients.

To estimate self-diffusion coefficients, different methodologies and corresponding models have been proposed in the literature. Unfortunately, most methods are specific to either liquid or gas states and to particular classes of substances. There is no widely accepted current theory capable of unifying the description of transport properties of the subcritical liquid, gas, and supercritical fluid states of any type of substance, independent of its chemical nature.

As a noticeable exception, the concept of entropy scaling¹⁴ is a semitheoretical approach that has taken a considerable step in this direction while maintaining valuable potential for industrial applications. As suggested by its name, this theory postulates that any given reduced transport property ($\tilde{\psi} = \psi/\psi_{\text{ref}}$) can be expressed as a function of the reduced residual entropy, denoted

Received: March 29, 2022

Revised: July 18, 2022

Accepted: July 22, 2022

Published: September 7, 2022



Table 1. Rosenfeld's Entropy Scaling Variables^{14,16} for Expressing the Self-Diffusion Coefficient in Dense States; ρ_N is the Number Density (Number of Molecules in a Volume Unit), m_0 is the Molecular Mass, and k_b is the Boltzmann Constant^a

entropy scaling variables	X-axis	Y-axis	$D_{\text{self}}^{\text{reference}}$	proposed model: for $\tilde{s}_{\text{TV-res}} \gtrsim 0.5$
expressions	$\tilde{s}_{\text{TV-res}} = -\frac{s_{\text{TV-res}}}{R}$	$\ln(\tilde{D}_{\text{self}}) = \ln\left(\frac{D_{\text{self}}^{\text{experimental}}}{D_{\text{self}}^{\text{reference}}}\right)$	$\rho_N^{-1/3} \sqrt{\frac{k_b T}{m_0}}$	$Y = -0.8X + \ln(0.6)$

^aFor illustration, Figure 1 shows the curve obtained when applying Rosenfeld's entropy scaling concept to the self-diffusion coefficient of pure methane and the diverging behavior that arises at low density when $\frac{s_{\text{TV-res}}}{R} \rightarrow 0$.

$\tilde{s}_{\text{TV-res}}$ and defined as the ratio of the residual entropy ($s_{\text{TV-res}}$) and the gas constant (R).¹⁵ For the sake of clarity, the notations used in the rest of this article are briefly commented upon. Reduced properties are topped by a tilde symbol (e.g., $\tilde{\psi}$) and defined as the ratio of the property ψ to a reference property ψ_{ref} obtained from a dimensional analysis and involving macroscopic variables (temperature, density, molecular mass, gas constant) and potentially microscopic parameters such as the collision diameter. This entropy scaling concept was originally developed by Rosenfeld¹⁴ through his work on simple theoretical fluids in dense states. He showed that when plotting the logarithm of shear viscosity and self-diffusion coefficient data, reduced in an appropriate way, against the reduced residual entropy $\tilde{s}_{\text{TV-res}}$, nearly universal linear laws were obtained. By universal, it is meant here that the law is the same for any type of substance. Later,¹⁶ he showed that the entropy scaling concept could be extended to a wider range of density domains, particularly the low-density region. These studies and the subsequent literature^{15,17–24} highlighted that the dependence between the logarithm of the reduced transport properties and the reduced residual entropy

- could be considered linear in specific domains but was nonlinear overall,
- was not universal, i.e., the curves were component-specific.

The formalism and the corresponding model for self-diffusion coefficients proposed by Rosenfeld¹⁶ are reviewed in Table 1.

Inspired by Rosenfeld's initial concept,^{14,16} several authors have proposed entropy scaling approaches for self-diffusion coefficients that mainly differ through the method used to reduce the transport property.

Addressing the case of atomic diffusion in condensed matter, Dzgutov²⁵ developed an expression for the $D_{\text{self}}^{\text{reference}}$ property derived from the Chapman–Enskog theory²⁶ by considering the Enskog collision rate. Therefore, in addition to the molecular density and temperature, $D_{\text{self}}^{\text{reference}}$ was also dependent on molecular descriptors such as the hard sphere diameter and the value of the radial distribution function at the contact distance. Subsequently, Bretonnet²⁷ considered the same reference term. In turn, Krekelberg et al.²⁸ derived a reference term by multiplying $[\rho D]_0$, the temperature-dependent product of the number density and diffusion coefficient of the considered species in dilute conditions, and the factor $\left(B + T \frac{dB}{dT}\right)$, where B is the second virial coefficient, resulting in an expression valid in low-density conditions. In the same spirit, Novak²⁹ used a reference term valid in dilute gas conditions, derived from the Chapman–Enskog theory, that involves molecular density and Lennard–Jones parameters such as a characteristic collision diameter, a characteristic energy of attraction between identical molecules and collision integrals. Novak's approach was to improve the description of the low-density region to prevent the divergent behavior shown in Figure 1. Although Novak's

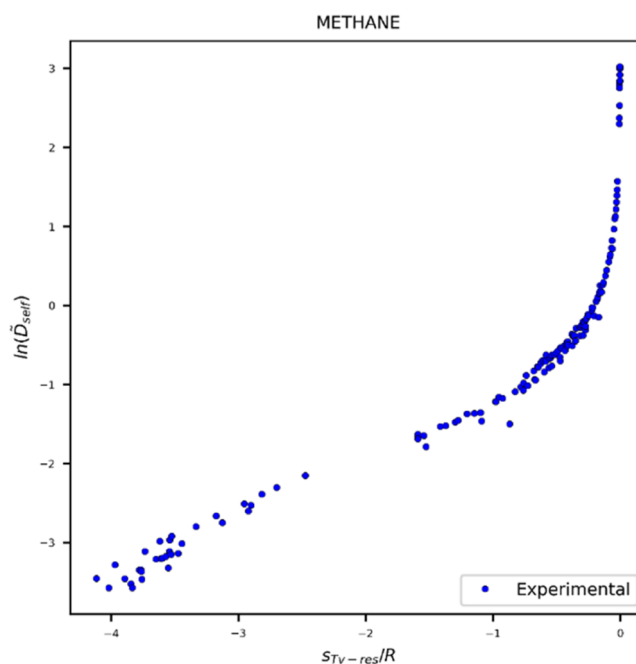


Figure 1. Rosenfeld's entropy scaling concept applied to the self-diffusion coefficient of pure methane.

proposal has been widely used recently to develop models for the prediction of transport properties of pure fluids^{19–21,30} and mixtures,²² there is currently no consensus on this approach. Indeed, it appeared that considering a $D_{\text{self}}^{\text{reference}}$ property valid in dilute gas conditions is not appropriate to describe liquids and dense gases. Nevertheless, it is worth noting that Novak's proposal made it possible to dramatically improve the modeling of low-density behavior.³¹

In contrast to the aforementioned studies, some authors have continued to apply Rosenfeld's initial reduction, such as Dyre and his isomorph theory³² as well as Bell's approach.^{17,33}

In a recent study of an entropy scaling formulation of the shear viscosity of a pure substance, we proposed a new general expression for the residual entropy variable and selected Rosenfeld's method for reducing the shear viscosity. Representing experimental data in this reduced space, V-shaped curves were systematically obtained, regardless of the considered compound, and strictly universal behavior was observed in the gaseous state. Using a rather simple functional form to correlate experimental data in the reduced space, good accuracy was achieved for different fluid states.¹⁵ Such a concept was recently applied to the correlation of thermal conductivities,³⁴ and deviations close to 3% between calculated and experimental data were obtained.

Building on this success, in this study, the same methodology is applied to self-diffusion coefficients to achieve the best formulation of the concept and thus to propose reliable models enabling the estimation of self-diffusion coefficients of a pure

fluid in the liquid, gas, and supercritical states. To estimate residual entropies and densities, the *I*-PC-SAFT³⁵ and translated^{36,37}-consistent^{38,39} Peng–Robinson (*tc*-PR⁴⁰) equations of state (EoSs) were used. The decision to consider two different EoSs, one belonging to the Van der Waals EoS family and the other belonging to the SAFT EoS family, is justified by (i) the industrial success of cubic EoSs and their excellent capacity to model the thermodynamic properties of any type of fluid⁴¹ and (ii) the remarkable ability of the *I*-PC-SAFT EoS, which does not embed an association term to model pure species,^{35,42} including polar and associating species. In such an EoS, the three molecular parameters (m , σ , and ϵ/k) are straightforwardly determined to exactly reproduce the experimental critical temperature, critical pressure, and acentric factor. The mathematical expressions of these two EoSs can be found elsewhere,^{35,40} but to fix the ideas, it seems important to recall that the average deviations between calculated and experimental data on a huge pure-component database containing more than 300 000 experimental data calculated with the *tc*-PR and *I*-PC-SAFT EoSs are, respectively, as small as 1.9 and 3.6%. In addition, the parameters required to use such EoSs are available in the open literature for thousands of pure components.^{41,42}

Use of the Entropy Scaling Concept to Correlate Self-Diffusion Coefficients. State of the Art. The *T_v*-residual entropy, denoted $s_{T_v\text{-res}}$ is a departure function expressing the difference between the entropy of a real fluid and that of a perfect gas at the same temperature and molar volume as the real fluid; it can be estimated using an equation of state in a straightforward manner.

From reasoning based on kinetic theory, Rosenfeld^{14,16} postulated that reduced self-diffusion coefficients could be expressed as a function of the reduced *T_v*-residual entropy. He introduced a so-called macroscopic reduction where D_{self} are divided by a temperature (T)- and a molecular density (ρ_N)-dependent term (here called the “reference property” and denoted $D_{\text{self}}^{\text{reference}}$) having the same dimension as the transport coefficient and reviewed in Table 1. Such a reduction is only suitable for dense-state fluids and for addressing dilute gas states. Rosenfeld derived a power-law dependence based on Enskog’s theory²⁶ but did not propose a relation unifying dense and dilute fluid states.

Our goal in this paper is to test the combination of the reference expression proposed by Rosenfeld for self-diffusion coefficients ($D_{\text{self}}^{\text{reference}}$) with the empirical entropy scaling X_{ES} -coordinate we recently developed to correlate shear viscosity¹⁵ and thermal conductivity³⁴ and for which promising results were obtained.

Building on the success obtained with the correlation of shear viscosities and thermal conductivities, our ambitions are to

- prevent the low-density divergence observed using Rosenfeld’s reduction (see Figure 1),
- obtain quasi-universal behavior at low density, and
- make the entropy scaling law less dependent on (i) the considered component and (ii) the EoS model selected to estimate density and residual entropy.

Such an entropy scaling (ES) X_{ES} -coordinate is defined as¹⁵

$$\begin{aligned} X_{\text{ES}} &= -\left(\frac{s_{T_v\text{-res}}}{s_{T_v\text{-res}}^c}\right) - \ln\left(\frac{s_{T_v\text{-res}}}{s_{T_v\text{-res}}^c}\right) \\ &= -\left(\frac{\tilde{s}_{T_v\text{-res}}}{\tilde{s}_{T_v\text{-res}}^c}\right) - \ln\left(\frac{\tilde{s}_{T_v\text{-res}}}{\tilde{s}_{T_v\text{-res}}^c}\right) \end{aligned} \quad (1)$$

and all of the details relative to the development of eq 1 can be found in our previous paper.¹⁵ In eq 1, $s_{T_v\text{-res}}^c$ is the critical value of the residual molar entropy. The key feature of this mathematical formulation is that the first term is dominant in dense fluid conditions, while the second term dominates at low density. We can thus expect to correlate self-diffusion coefficients with a unique mathematical expression regardless of the fluid state (liquid, gas, or supercritical). Furthermore, as another important feature of introducing this new X_{ES} variable, \tilde{D}_{self} becomes a linear function of X_{ES} when $X_{\text{ES}} \rightarrow +\infty$. This particularly interesting feature is illustrated in Figure 2.

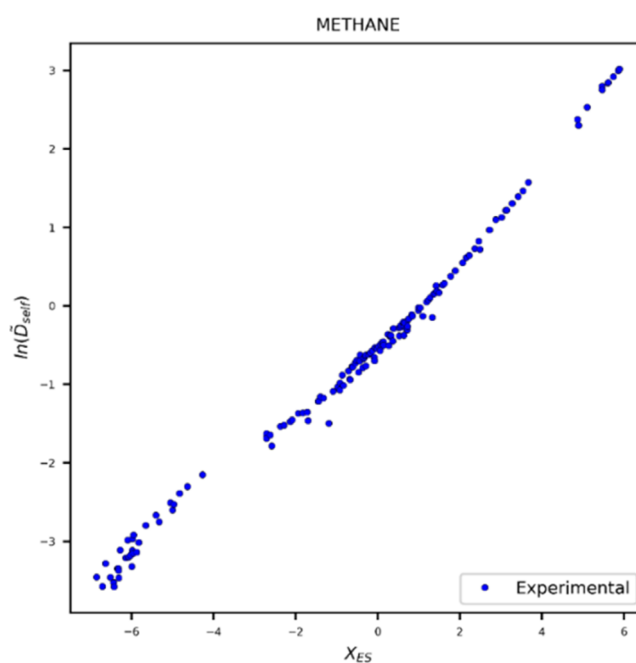


Figure 2. Illustration of the entropy scaling formulation proposed in this study to model the self-diffusion coefficient of methane. *T_v*-residual entropies and density values were calculated using the *I*-PC-SAFT³⁵ EoS.

In agreement with our expectations, Figure 2 shows that the liquid- and gas-like states align along a single curve in the (Y_{ES} , X_{ES}) plane. For better visualization of the distribution of the various pressure and temperature conditions, Figure 3 shows characteristic vapor–liquid saturation curves as well as a series of liquid, gas, and supercritical branches of various isotherms for the case of methane modeled with the *I*-PC-SAFT EoS.³⁵ These curves are represented in (P_r , Y_{ES} , X_{ES}) space (see Figure 3A), where $P_r = P/P_c$ denotes the reduced pressure and $Y_{\text{ES}} = \ln(\tilde{D}_{\text{self}})$ is the natural logarithm of the reduced self-diffusion coefficient (following Rosenfeld’s definition), in the (P_r , X_{ES}) plane (Figure 3B) and in the (Y_{ES} , X_{ES}) plane (Figure 3C).

Search for a Functional Form for Describing the Relationship between the Self-Diffusion Coefficient and Residual Entropy Variable. Figure 2 shows that the reduced self-diffusion coefficient monotonically increases from dense to dilute fluids, i.e., when density decreases. It was, however, observed that the

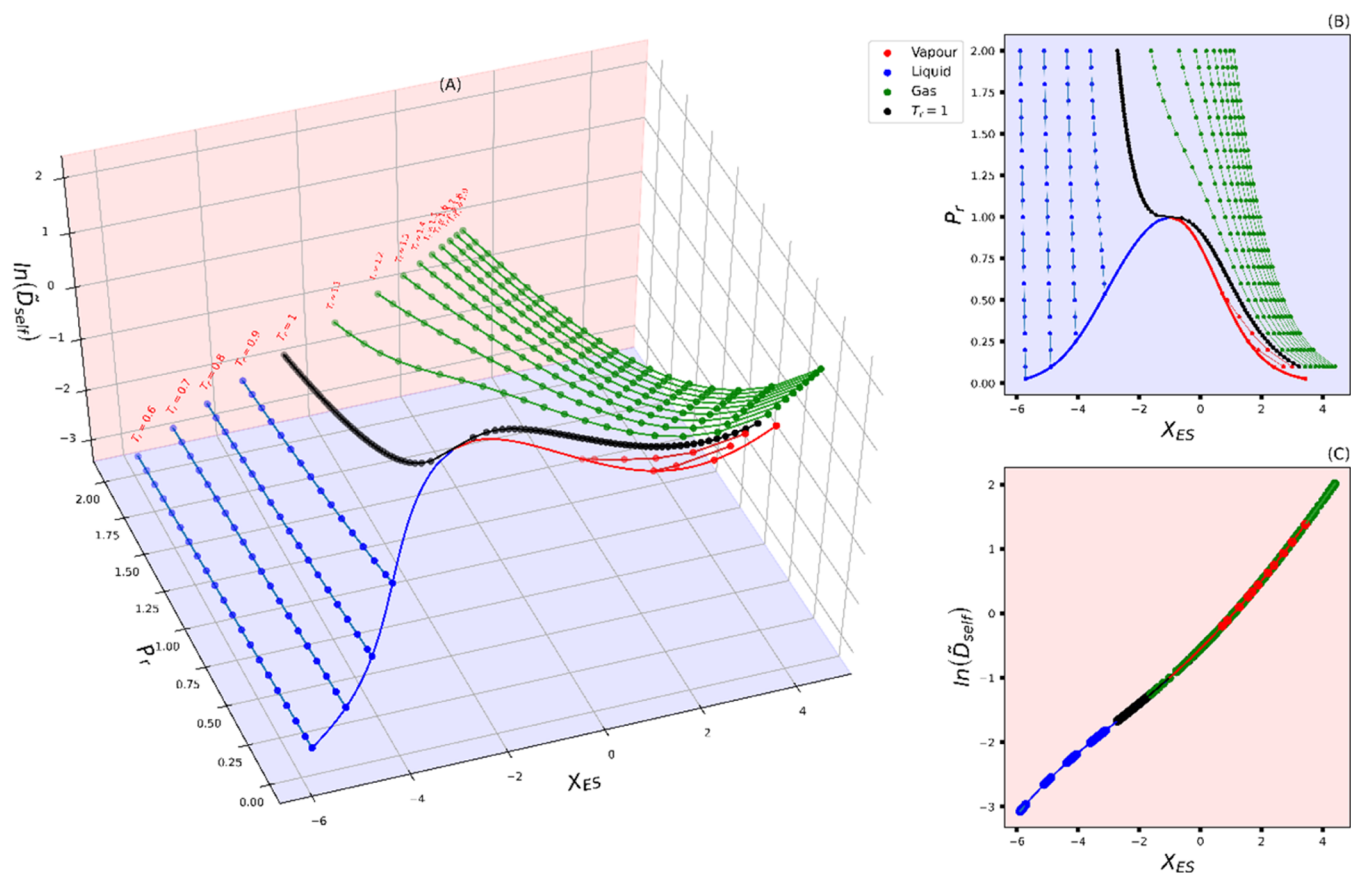


Figure 3. Graphical illustration of the entropy scaling formulation proposed here through the representation of isotherms and saturation curves of pure methane in three different diagrams. The reduced temperatures of the isotherms are in the range of $T_r = 0.6$ – 1.9 , while the reduced pressures are in the range of $P_r = 0.1$ – 2 . (A) Representation in the (P_r, Y_{ES}, X_{ES}) space, (B) representation in the (P_r, X_{ES}) plane, and (C) representation in the (Y_{ES}, X_{ES}) plane.

dependence of the self-diffusion coefficients on density, i.e., from low ($X_{ES} < 0$) to high density ($X_{ES} < 0$), changes severely with fluid conditions (temperature and pressure). In diagrams reporting $Y_{ES} = \ln(\tilde{D}_{self})$ vs X_{ES} , this dependence cross-over induces

- component-dependent curve slopes and
- nonlinear behavior from moderately dense ($X_{ES} \approx 0$) to dense fluids ($X_{ES} \ll 0$).

To satisfactorily capture those mass transport regimes and maintain a high degree of flexibility of the functional form for the prediction of the self-diffusion coefficients, it is proposed here to keep the same expression as the one previously used for shear viscosity, eq 2

$$\ln(\tilde{D}_{self})_{calc} = f_{dense}(\tilde{s}_{T_v-res}) \times g_{dense} + f_{gas}(\tilde{s}_{T_v-res}) \times g_{gas} + d \quad (2)$$

where f_{dense} and f_{gas} are functions describing the dense-state behavior (i.e., for $X_{ES} < 0$; note that the term “dense” concerns both subcritical liquid and supercritical fluids) and dilute gas behaviors (i.e., for $X_{ES} > 0$; the term “gas” means both subcritical and supercritical fluids); g_{dense} and g_{gas} are damping factors making f_{dense} dominant in the dense region, and conversely, f_{gas} dominant in the gas region; and d is a component-specific constant. The following expressions are introduced to express these various quantities

$$\left\{ \begin{aligned} f_{dense}(\tilde{s}_{T_v-res}) &= (a_1 + a_2 \tilde{s}_{T_v-res} + a_3 \tilde{s}_{T_v-res}^2) X_{ES} \\ g_{dense} &= \frac{1}{1 + e^{cX_{ES}}} \\ f_{gas}(\tilde{s}_{T_v-res}) &= b X_{ES} \\ g_{gas} &= \frac{1}{1 + e^{-cX_{ES}}} \end{aligned} \right. \quad (3)$$

In eq 3, (a_1, a_2, a_3) , b , c , and d are six adjustable parameters. Therefore, the final model proposed here is

$$\left\{ \begin{aligned} \ln\left(\frac{D_{self}}{D_{self}^{reference}}\right)_{calc} &= \left[\frac{a_1 + a_2 \tilde{s}_{T_v-res} + a_3 \tilde{s}_{T_v-res}^2}{1 + e^{cX_{ES}}} \right] \\ &+ \left[\frac{b}{1 + e^{-cX_{ES}}} \right] X_{ES} + d \\ \text{with: } D_{self}^{reference} &= \rho_N^{-1/3} \sqrt{\frac{k_b T}{m_0}} \\ \text{and } X_{ES} &= -\left(\frac{s_{T_v-res}}{s_{T_v-res}^c}\right) - \ln\left(\frac{s_{T_v-res}}{s_{T_v-res}^c}\right) \end{aligned} \right. \quad (4)$$

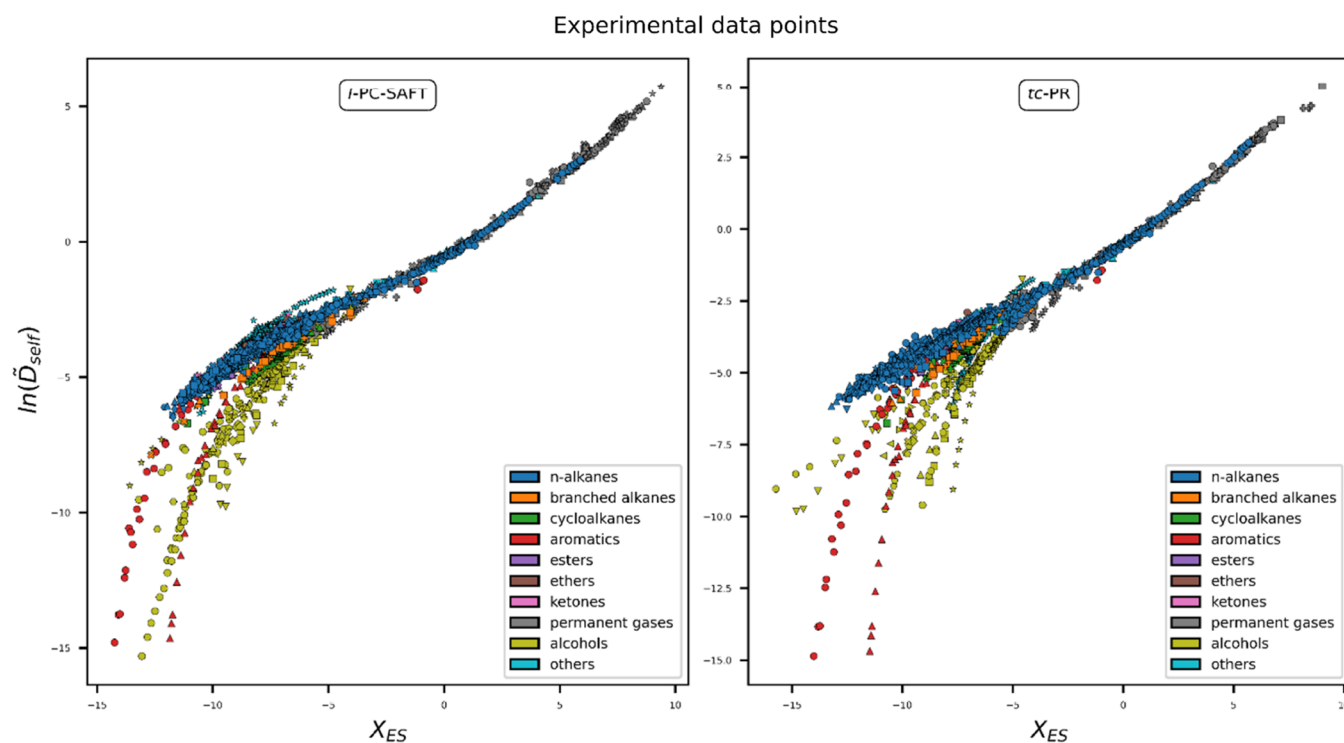


Figure 4. Overview of all experimental data in the $\ln(\tilde{D}_{\text{self}})$ vs X_{ES} plane. The thermodynamic properties involved in the definition of \tilde{D}_{self} and X_{ES} were estimated using the *I*-PC-SAFT EoS (left panel) and the *tc*-PR EoS (right panel). Each color corresponds to a specific chemical family, and each symbol corresponds to a specific compound.

The calculated Tv-residual entropies and density values are EoS-dependent, so that the adjusted parameters are specific to each considered EoS.

METHODS, RESULTS, AND DISCUSSION

Methodology for Model Derivation. To develop our entropy scaling-based models for the estimation of self-diffusion coefficients, ~2400 subcritical gas, subcritical liquid, and supercritical data associated with 72 pure substances were considered. All of these data were extracted from the database of self-diffusion coefficient measurements proposed by Suárez-Iglesias et al.¹³ This database was selected because it serves as a reference for comparing models that correlate self-diffusion coefficients. It, however, could be extended by adding many molecular dynamics simulation data recently published.^{23,43–46} The many data are graphically represented in Figure 4 and are used to determine the sets of parameters a_1 , a_2 , a_3 , b , c , and d by minimizing the following objective function

$$F_{\text{obj}}^{D_{\text{self}}} = \frac{100}{Nb_{\text{data}}} \sum_{i=1}^{Nb_{\text{data}}} 0.5 \times \left(\left| \frac{D_{\text{self},i}^{\text{calc}} - D_{\text{self},i}^{\text{exp}}}{D_{\text{self},i}^{\text{exp}}} \right| + \left| \frac{Y_{\text{ES},i}^{\text{calc}} - Y_{\text{ES},i}^{\text{exp}}}{Y_{\text{ES},i}^{\text{exp}}} \right| \right) \quad (5)$$

where Nb_{data} is the total number of data taken into account, $Y_{\text{ES},i}^{\text{calc}}$ and $Y_{\text{ES},i}^{\text{exp}}$ are the logarithm of the experimental and calculated (according to eq 5) values of the reduced self-diffusion coefficient at the given temperature and pressure of data point i , and $D_{\text{self},i}^{\text{exp}}$ and $D_{\text{self},i}^{\text{calc}}$ are the equivalent experimental and calculated values of the self-diffusion coefficient, respectively. Equation 5 averages the relative deviations on the self-diffusion

coefficient (D_{self}) and also on $Y_{\text{ES}} = \ln(\tilde{D}_{\text{self}})$. The mean absolute percentage error (MAPE) on D_{self} is included in eq 5 since our primary objective is to accurately model the self-diffusion coefficients. The MAPE on Y_{ES} was added to help the convergence of the minimization procedure. Since the self-diffusion coefficient undergoes an increase of several orders of magnitude (e.g., from 10^{-9} in dense states to 10^{-5} in dilute states for the case of methane), the consideration of the logarithm of the reduced coefficient, which evolves under values of the same order of magnitude (from -4 to 4 for methane), ensures that errors in both the dilute state and the dense state have a similar impact on the optimization procedure. Notably, some experimental data points were removed from the database after application of the following filters

- Data associated with pressures outside of the range [10^{-3} MPa; 10^2 MPa] were considered (i) potentially inaccurate and (ii) outside of the pressure range for most applications. Therefore, they were discarded.
- To eliminate out-of-chart data, the absolute deviation $\Delta Y_i = |Y_{\text{ES},i}^{\text{calc}} - Y_{\text{ES},i}^{\text{exp}}|$ was calculated for each data point and compared to the average deviation $\Delta \bar{Y}$ estimated for the species under consideration. Data such that $\Delta Y_i > \Delta \bar{Y} + 3\sigma$ (where σ denotes the standard deviation, and $\Delta \bar{Y}$, the MAPE on Y_{ES}) were discarded. As a double check, it was verified graphically that each datum eliminated by the test deviated strongly from the general trend and could be considered an outlier.
- For the case of the *tc*-PR-based model, data at temperatures above $4 \cdot T_c$ (with T_c , the critical temperature of the pure fluid considered) were discarded because it was observed previously that the cubic EoS may fail to predict Tv-residual entropy in this specific temperature range. Notably, however, the quasi-totality of practical

applications uses temperatures much lower than $4T_c$. For more details, the reader is referred to our previous work dealing with the modeling of shear viscosity.¹⁵

The minimization procedure was based on the Broyden–Fletcher–Goldfarb–Shanno (BFGS) algorithm, a quasi-Newton optimization method. To ensure the consistency of the optimized parameter sets, it was necessary to verify that the algorithm converged to global (i.e., nonlocal) minima. To do so, multiple initialization sets were systematically generated using a random process for each compound. Among all of the parameter sets returned by the routine, the optimal one was identified as follows

- At least half of the initial guesses led to the same optimal parameter set.
- This parameter set was associated with the lowest objective function value and a nearly zero gradient norm.

Universal Behavior for Dilute Gas. As observed in Figure 4, dilute gases characterized by low-density conditions (ρ_N close to zero or, equivalently, positive X_{ES} values) exhibit quasi-universal behavior, and it is proposed to mathematically model this behavior. Under low-density conditions, the model proposed in this paper (see eq 4) can be approximated by

$$\ln\left(\frac{D_{\text{self}}}{D_{\text{self}}^{\text{reference}}}\right)_{\text{calc}} \underset{\rho_N \rightarrow 0}{\sim} \left(\frac{b}{1 + e^{-cX_{ES}}}\right)X_{ES} + d \quad (6)$$

From a graphical point of view

- b is the slope of the asymptote arising at $X_{ES} \gg 0$;
- c characterizes the sharpness of the transition between the dense and dilute parts of the (Y_{ES}, X_{ES}) curve; and
- d is the Y_{ES} value at the origin ($X_{ES} = 0$).

According to eq 4, parameters c and d affect the representation of dense fluid data, i.e., they influence the modeling of data at $X_{ES} < 0$. It is thus impossible to estimate universal values of parameters b , c , and d (denoted b_{univ} , c_{univ} , d_{univ} hereafter) by considering dilute gas data only. For this reason, data for the dense state were included in the fitting procedure aimed at determining b_{univ} , c_{univ} , and d_{univ} . n -Alkanes experimental data in the dense state were considered (and data for all of the other molecules were excluded) because Figure 4 shows that n -alkanes have nearly universal behavior in the dense region. In other words, it is a satisfactory approximation to use the same a_i coefficients ($i = 1, 2, 3$) for all of the n -alkanes in eq 4. In summary, parameters b_{univ} , c_{univ} , and d_{univ} as well as a_i coefficients for n -alkanes, were fitted against (i) dilute gas data ($X_{ES} > 0$) of all of the compounds for which such data were available and (ii) dense liquid n -alkane data. The results are reported in Table 2 where four digits were necessary to obtain a stabilized value of the objective function that was minimized.

Parametrization Strategy 1: Use of Component-Specific Parameters. In this section, parameters a_i ($i = 1, 2,$

Table 2. Universal Parameters for the Self-Diffusion Model in the Dilute Gas Region ($X_{ES} \geq 0$) Associated with Two Different EoS (Used for Estimating Density and Residual Entropy), Namely, the I -PC-SAFT and tc -PR Models

parameter	I -PC-SAFT EoS	tc -PR EoS
b_{univ}	0.6686	0.6190
c_{univ}	0.2861	0.4993
d_{univ}	−0.5451	−0.5151

3), b , c , and d of eq 4 were determined for all pure substances for which this determination was possible.

Notably, when experimental data were lacking in the dilute gas regions, parameters b , c , and d were set to b_{univ} , c_{univ} , and d_{univ} , respectively (Table 2). More generally, the estimation of component-specific parameters (i.e., a_1, a_2, a_3) [and (b, c, d) when possible] was performed as follows

- (1) If at least five experimental data points were available in the dense state ($X_{ES} < 0$) and at least three experimental data points were simultaneously available in the dilute gas region ($X_{ES} \geq 0$), then specific parameters a_1, a_2, a_3 and b, c, d were fitted to these data.
- (2) If at least five experimental data points were available in the dense state ($X_{ES} < 0$) and fewer than three experimental data points were available in the dilute gas region ($X_{ES} \geq 0$), then the specific parameters $a_1, a_2,$ and a_3 were fitted to these data, whereas $b, c,$ and d are fixed to the universal values.
- (3) If less than five experimental data points were available at the dense state ($X_{ES} < 0$), no parameters were fitted (the component was disregarded, and no deviations with experimental data were calculated), but universal $b, c,$ and d parameters were used to predict self-diffusion coefficients in the dilute gas region.

Two sets of component-specific parameters were determined for 72 chemical species, one to be used with the I -PC-SAFT EoS and the second with the tc -PR EoS. The EoSs were used for estimating thermodynamic properties: density and residual entropy. Numerical values of these parameters along with the deviations in terms of density and vapor pressure are available in the Supporting information. Detailed Excel sheets containing the experimental values and the values of the self-diffusion coefficients calculated with both considered EoSs are also provided as additional Supporting information for facilitated use and analysis. Figure 5 provides a graphical overview of the achieved results. Similar accuracies in the correlation of self-diffusion coefficients were obtained using either the I -PC-SAFT EoS (MAPE on $D_{\text{self}} = 7.5\%$) or the tc -PR EoS (MAPE = 7.9%), with a slight advantage for the I -PC-SAFT model.

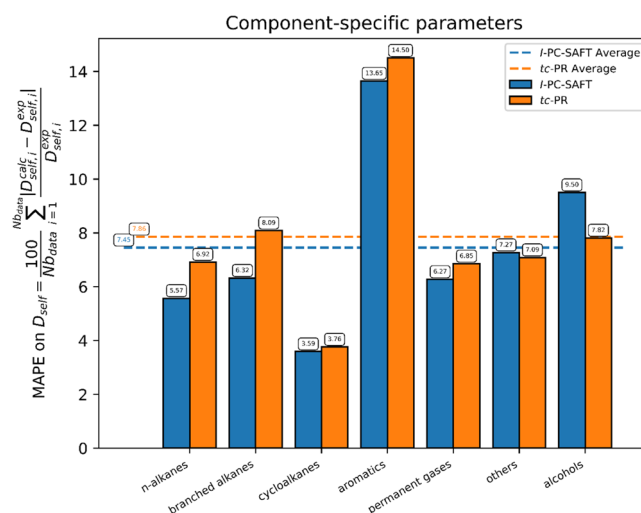


Figure 5. Correlation of self-diffusion coefficients using the model given by eq 4 and parametrization strategy 1 (component-specific parameters). Summary of the MAPEs obtained using either the I -PC-SAFT or the tc -PR EoS for estimating density and residual entropy.

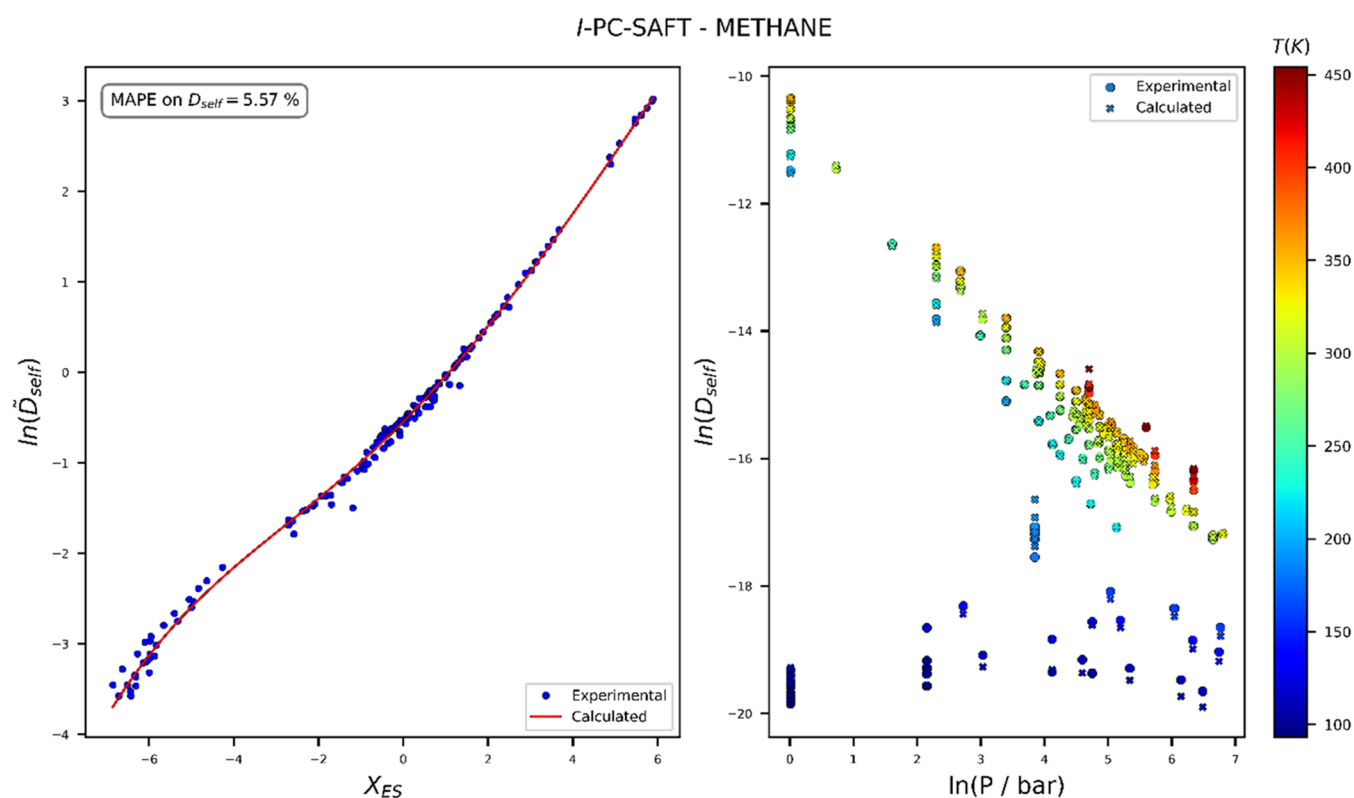


Figure 6. Application of the entropy scaling (ES)-based model combining eq 4 and parametrization strategy 1 to methane using the *I*-PC-SAFT EoS to estimate density and residual entropy. Left panel: (X_{ES} , Y_{ES}) plane. Right panel: self-diffusion coefficient vs pressure (log–log scale).

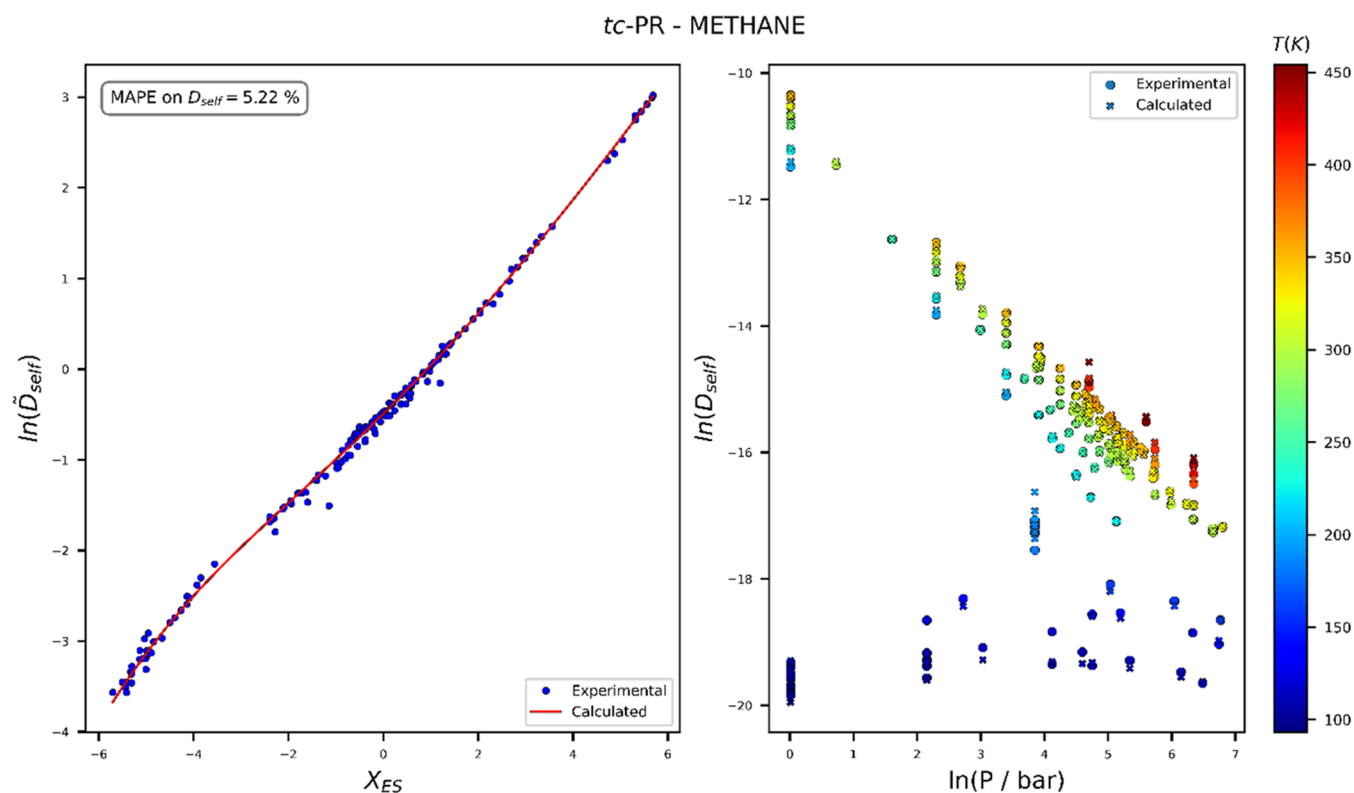


Figure 7. Application of the ES-based model combining eq 4 and parametrization strategy 1 to methane using the *tc*-PR EoS (for more details, refer to the caption of Figure 6).

Examples of results obtained with the model described by eq 4 and parametrization strategy 1 (component-specific param-

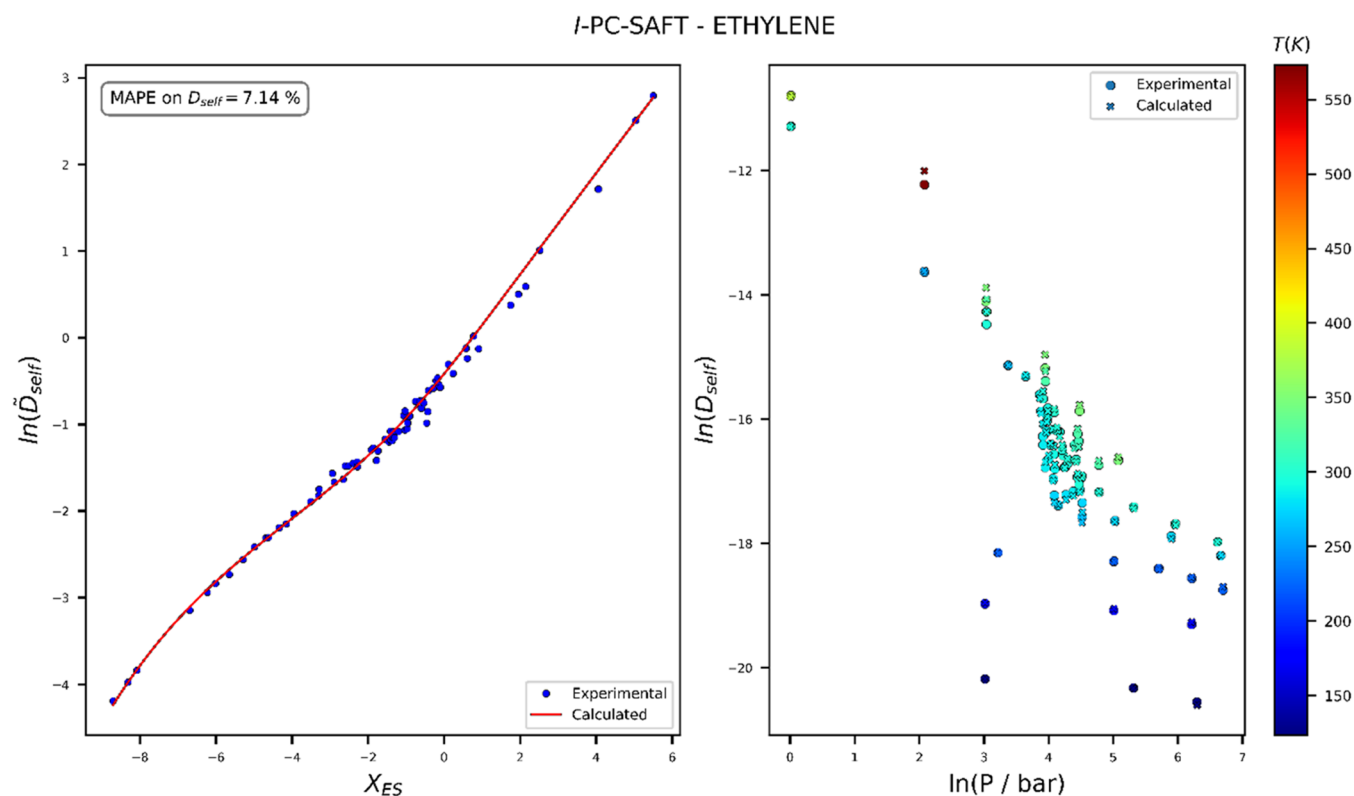


Figure 8. Application of the ES-based model combining eq 4 and parametrization strategy 1 to ethylene using the *I*-PC-SAFT EoS (for more details, refer to the caption of Figure 6).

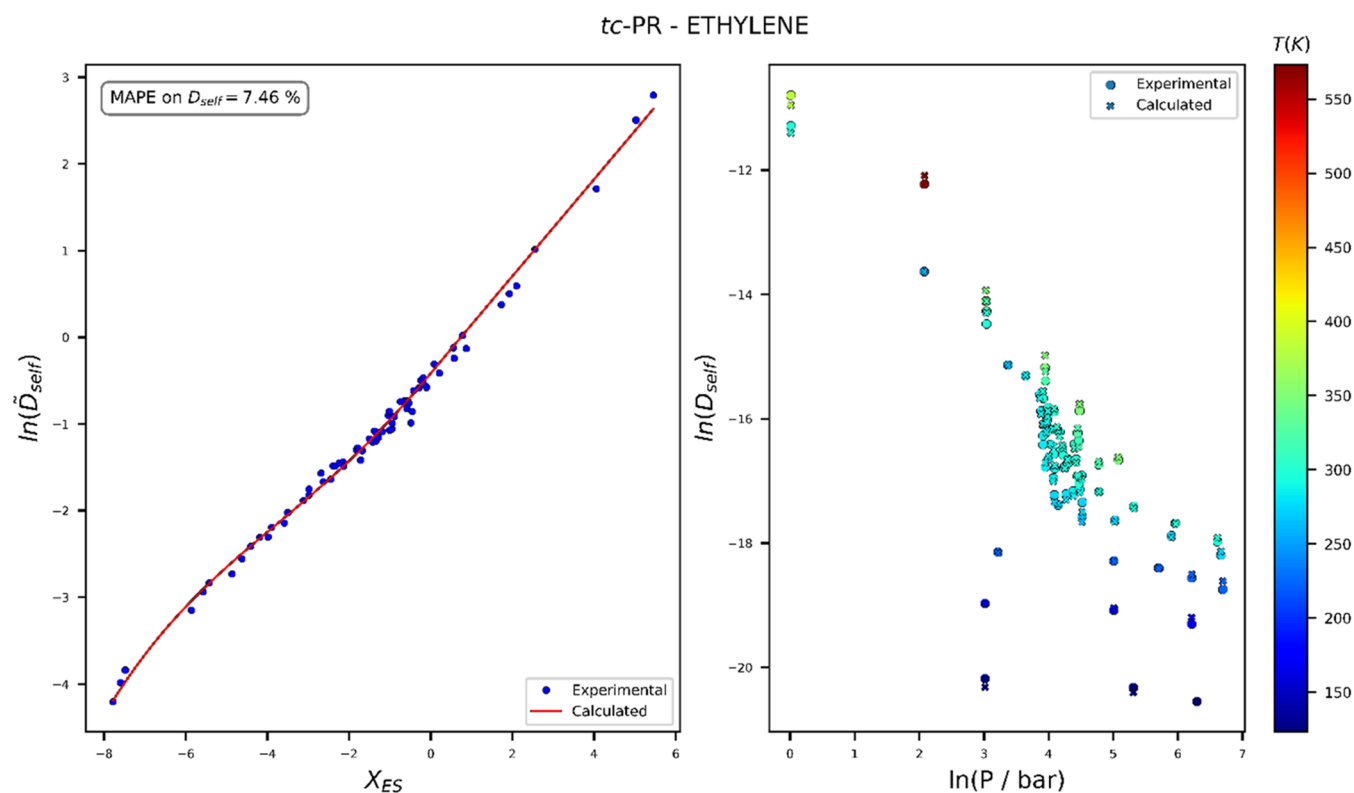


Figure 9. Application of the ES-based model combining eq 4 and parametrization strategy 1 to ethylene using the *tc*-PR EoS (for more details, refer to the caption of Figure 6).

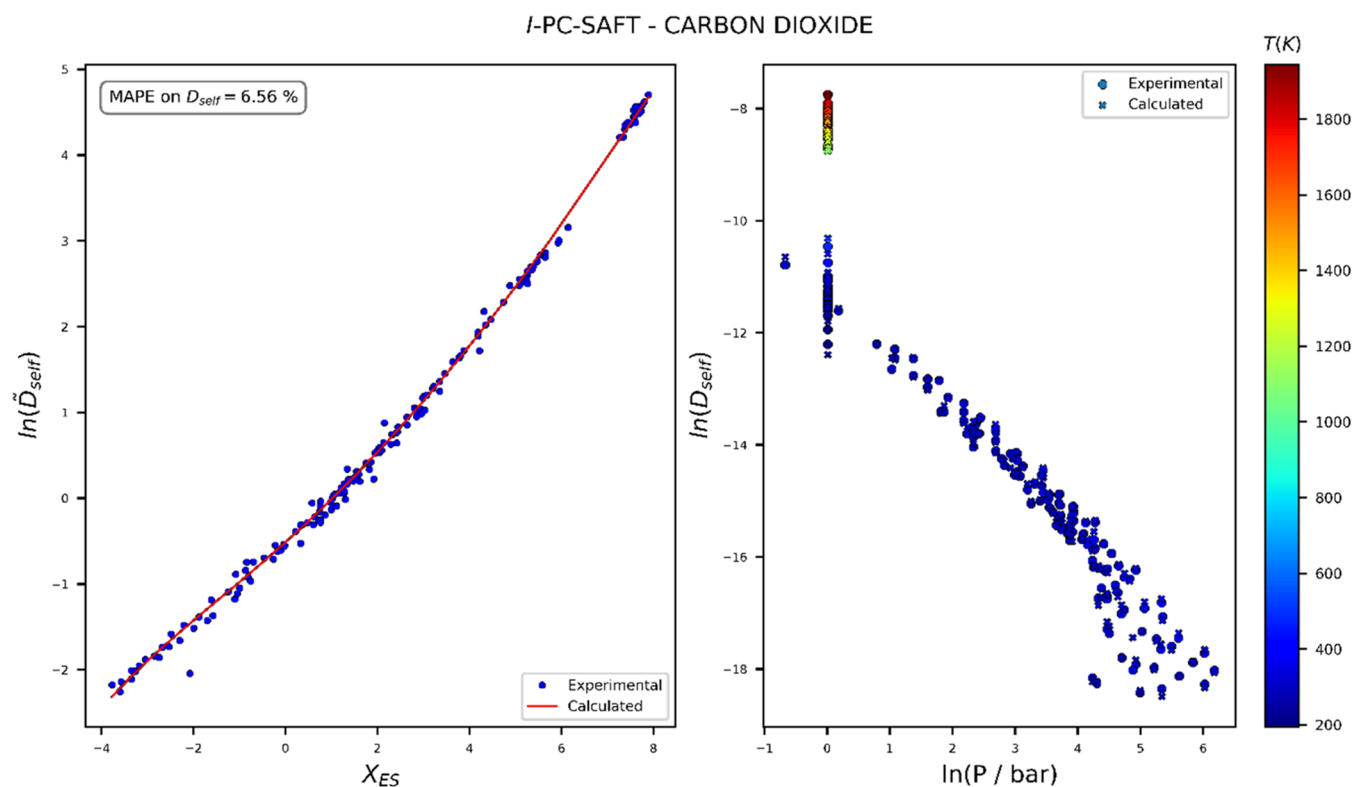


Figure 10. Application of the ES-based model combining eq 4 and parametrization strategy 1 to CO₂ using the *I*-PC-SAFT EoS (for more details, refer to the caption of Figure 6).

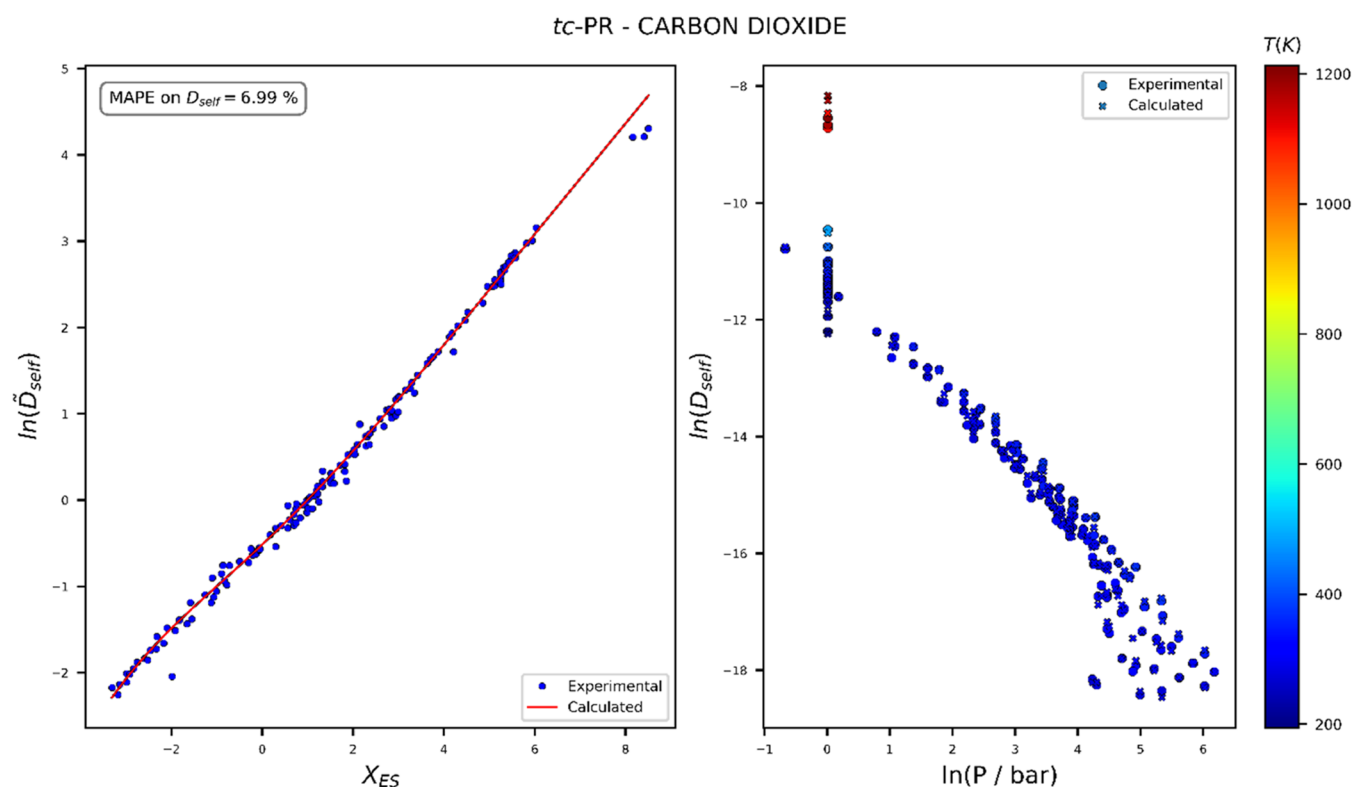


Figure 11. Application of the ES-based model combining eq 4 and parametrization strategy 1 to CO₂ using the *t*_c-PR EoS (for more details, refer to the caption of Figure 6).

ters) are provided in Figures 6–13 in the (X_{ES} , Y_{ES}) and ($\ln(D_{self})$, $\ln P$) planes for both the *I*-PC-SAFT- and *t*_c-PR-based models.

As can be observed from Figures 6–13, parametrization strategy 1 (PS1) proposed here enables us to achieve a quite reasonable description of the self-diffusion coefficients. Similar

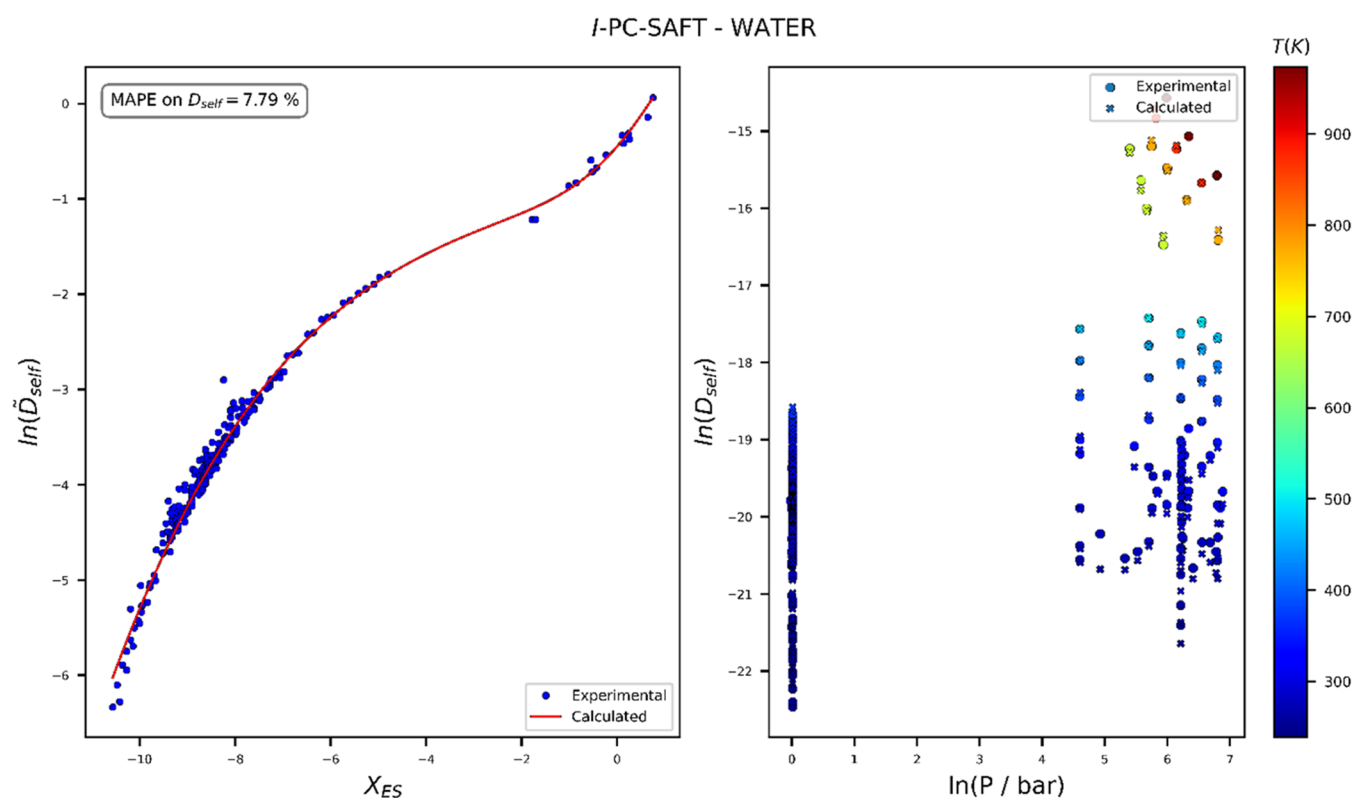


Figure 12. Application of the ES-based model combining eq 4 and parametrization strategy 1 to water using the *I*-PC-SAFT EoS (for more details, refer to the caption of Figure 6).

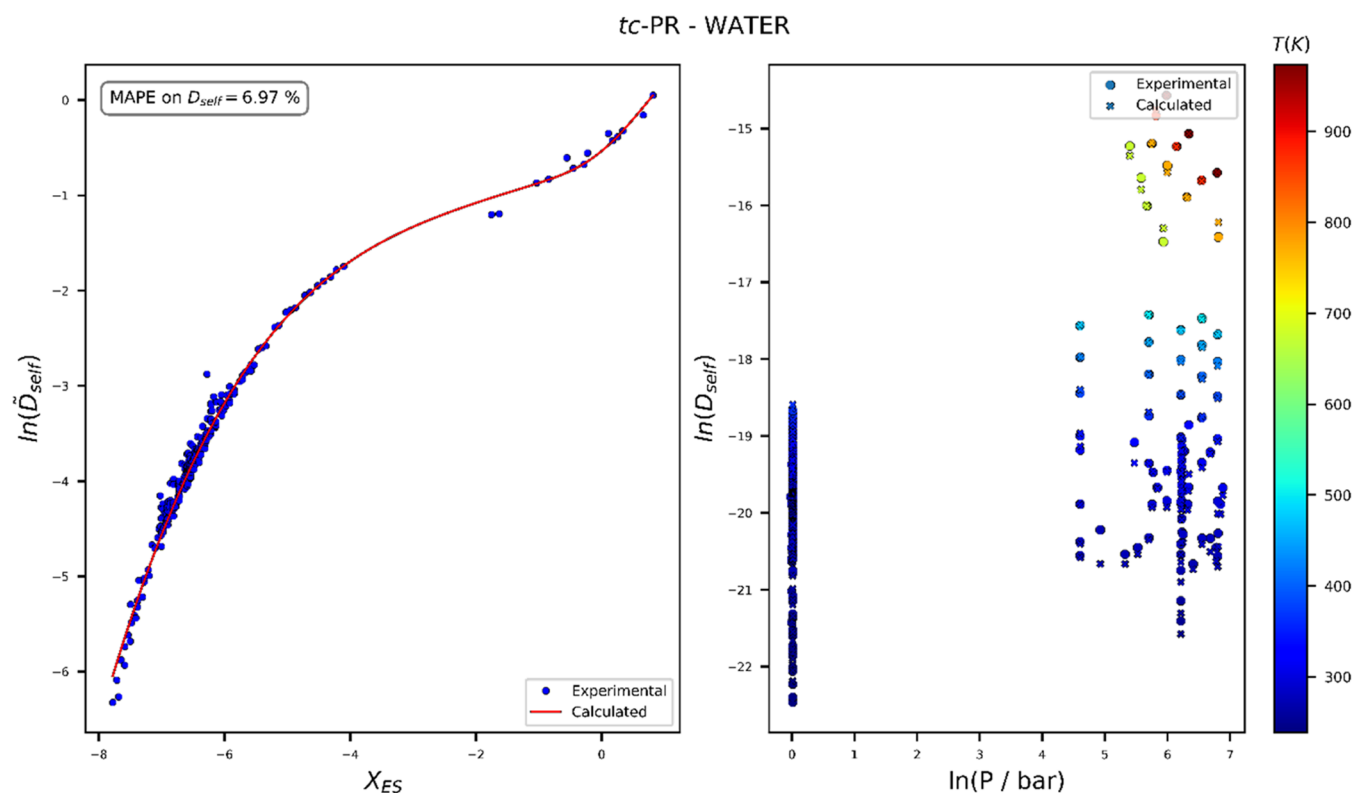


Figure 13. Application of the ES-based model combining eq 4 and parametrization strategy 1 to water using the *tc*-PR EoS (for more details, refer to the caption of Figure 6).

accuracy is obtained with both the *I*-PC-SAFT- and *tc*-PR-based models, from dense liquid to dilute gas conditions, by including

supercritical states. Considering measurement uncertainties,¹³ which are relatively more important for self-diffusion coefficients

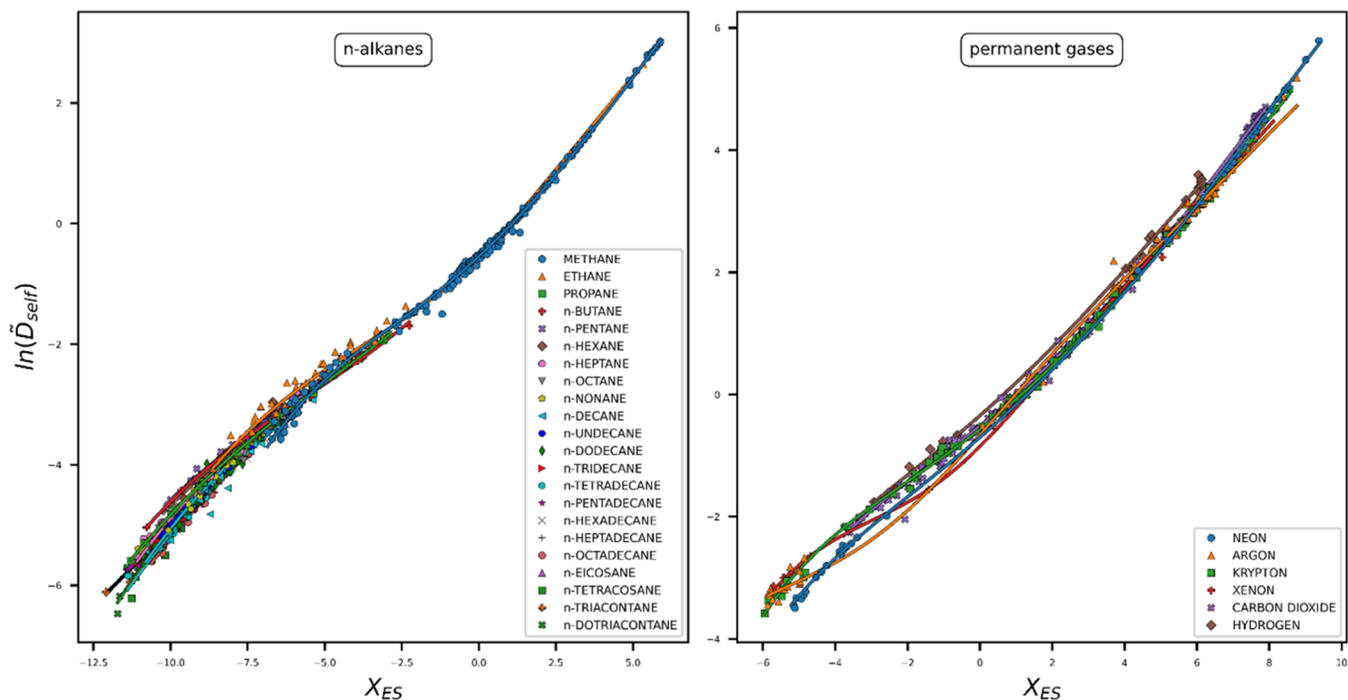
I-PC-SAFT - component-specific parameters

Figure 14. Application of the ES-based model combining eq 4 and parametrization strategy 1 to *n*-alkanes and permanent gases using the *I*-PC-SAFT EoS. Points: experimental data; solid line: model.

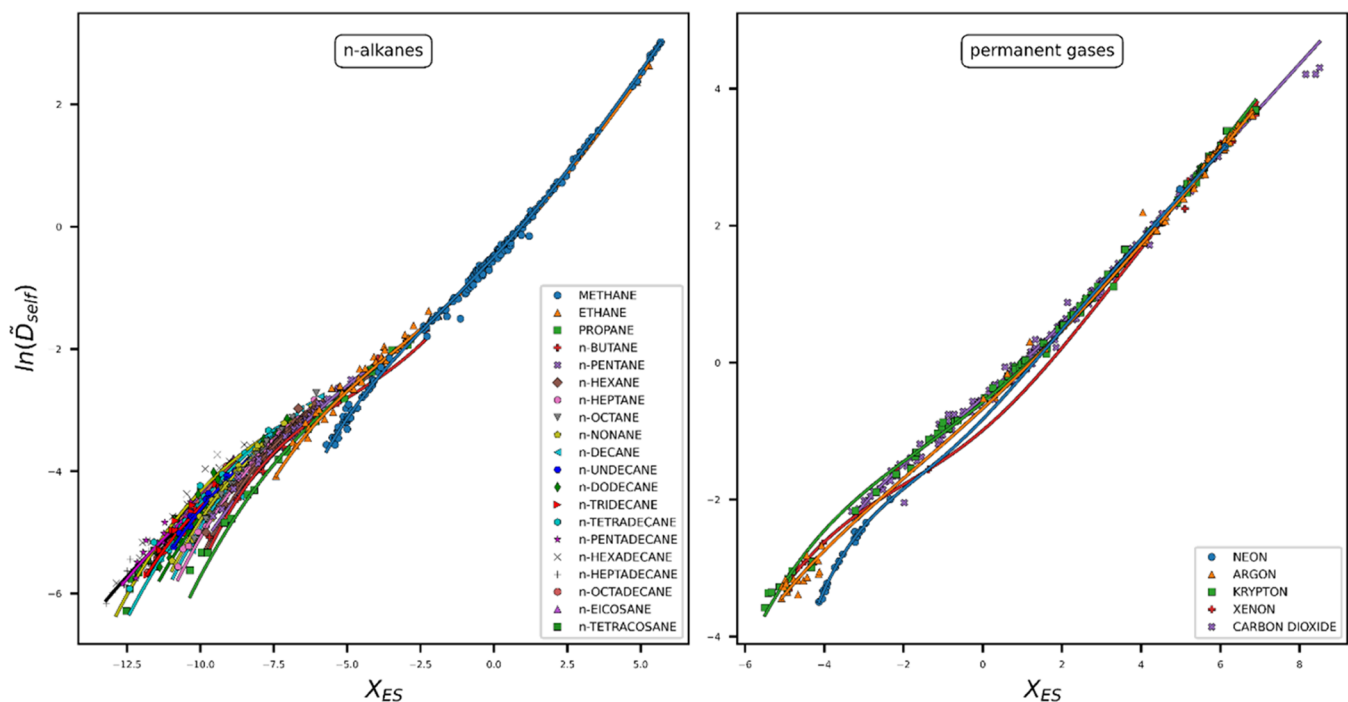
tc-PR - component-specific parameters

Figure 15. Application of the ES-based model combining eq 4 and parametrization strategy 1 to *n*-alkanes and permanent gases using the *tc*-PR EoS. Points: experimental data; solid line: model.

than for shear viscosities, it can be concluded that the flexibility of the functional form proposed here allows an accurate description of the self-diffusion coefficient regardless of the chemical species of interest. Notably, the use of universal

parameters in the low-density region makes it possible to overcome the absence of experimental data for dilute gas.

For water, which is a fluid acknowledged as complex and difficult to model, accurate results are obtained, as shown by Figures 12 and 13 (MAPE on $D_{\text{self}} \sim 7\%$) although the two EoS

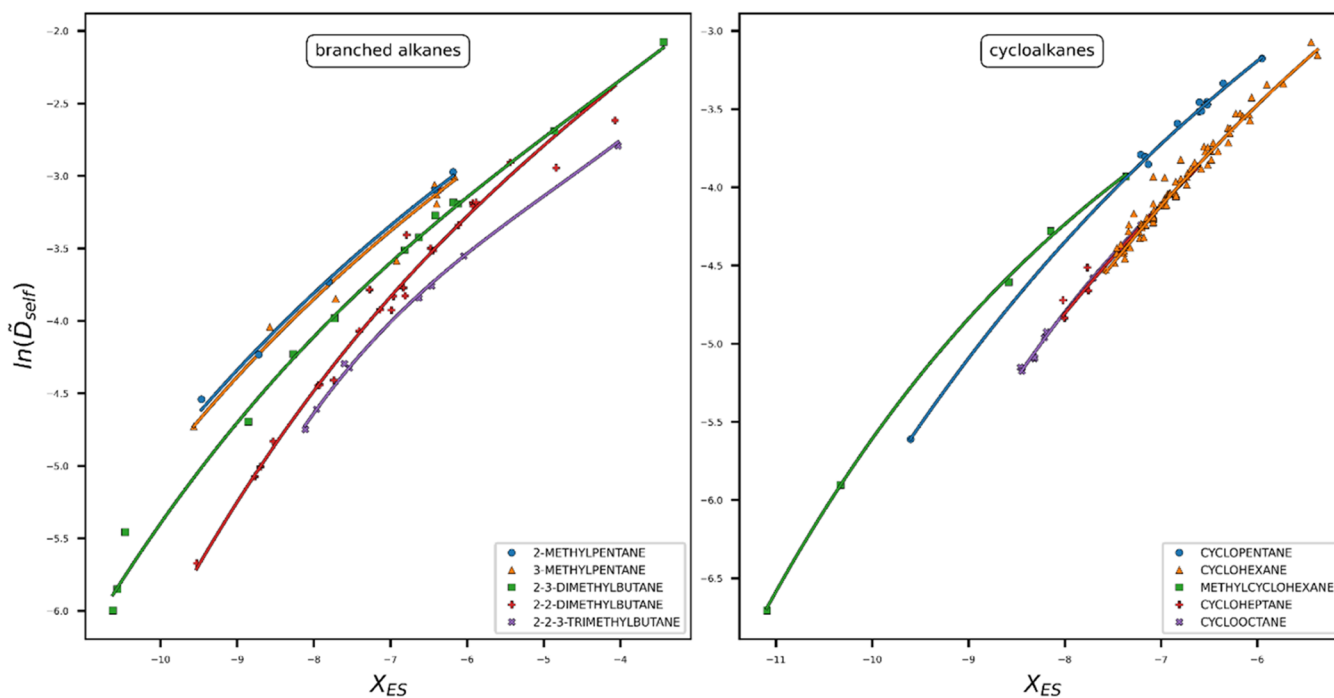
I-PC-SAFT - component-specific parameters

Figure 16. Application of the ES-based model combining eq 4 and parametrization strategy 1 to branched alkanes and cycloalkanes using the *I*-PC-SAFT EoS. Points: experimental data; solid line: model.

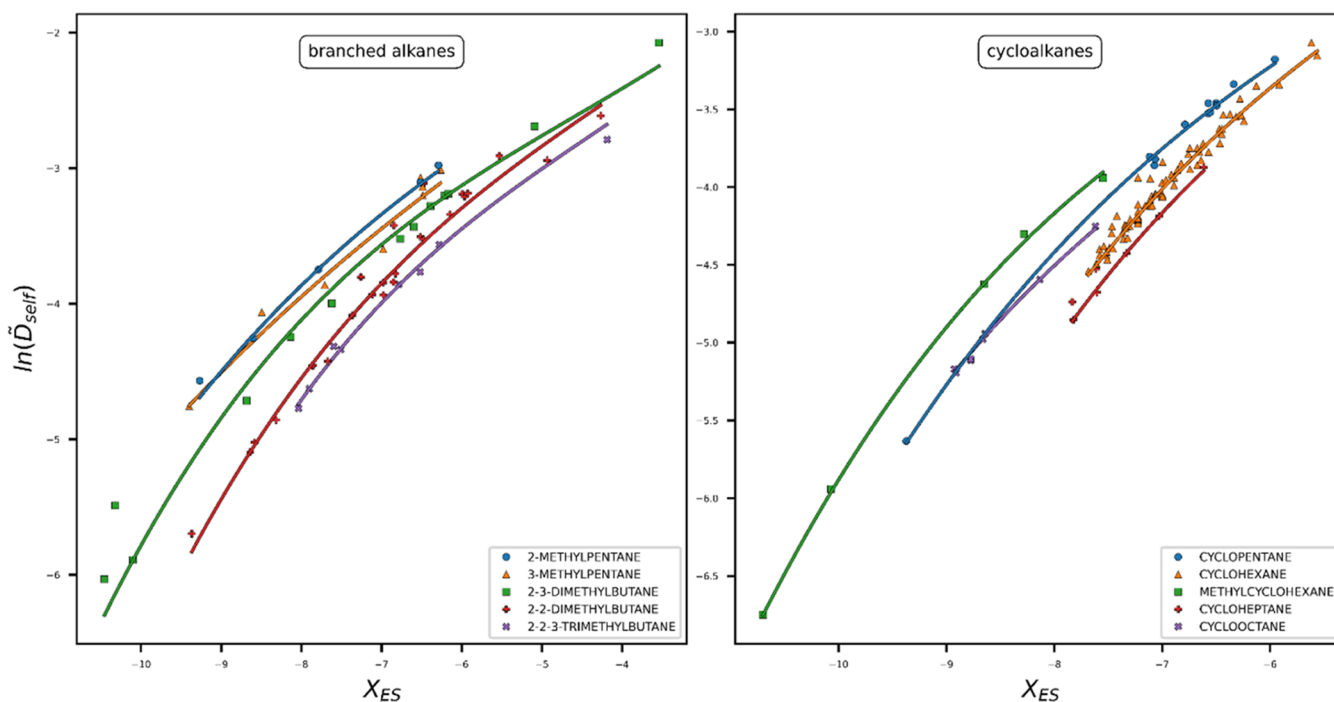
tc-PR - component-specific parameters

Figure 17. Application of the ES-based model combining eq 4 and parametrization strategy 1 to branched alkanes and cycloalkanes using the *tc*-PR EoS. Points: experimental data; solid line: model.

do not embed an association term. To provide a broad and fair overview of PS1 capacities, Figures 14–17 show the results obtained for the nonpolar and nonassociating molecules, that is, *n*-alkanes, permanent gases, branched alkanes, and cycloalkanes. Figures 18 and 19 show the results obtained for *n*-alcohols and

aromatic compounds that contain polar and/or associating chemical groups (through hydrogen bonding or pi-stacking). Alcohols are correlated with a deviation close to 10% which is excellent if we consider the scatter of the experimental data points. Such a result demonstrates that the proposed model can

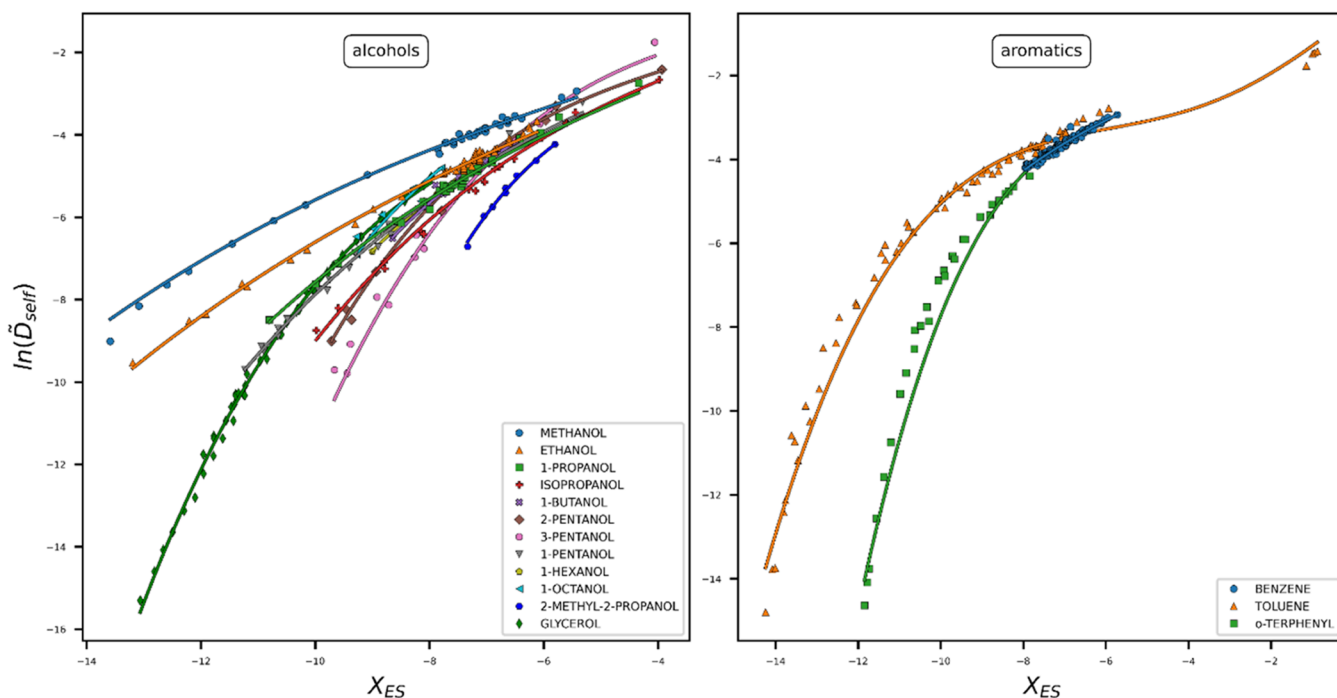
I-PC-SAFT - component-specific parameters

Figure 18. Application of the ES-based model combining eq 4 and parametrization strategy 1 to *n*-alcohols and aromatic compounds using the *I*-PC-SAFT EoS. Points: experimental data; solid line: model.

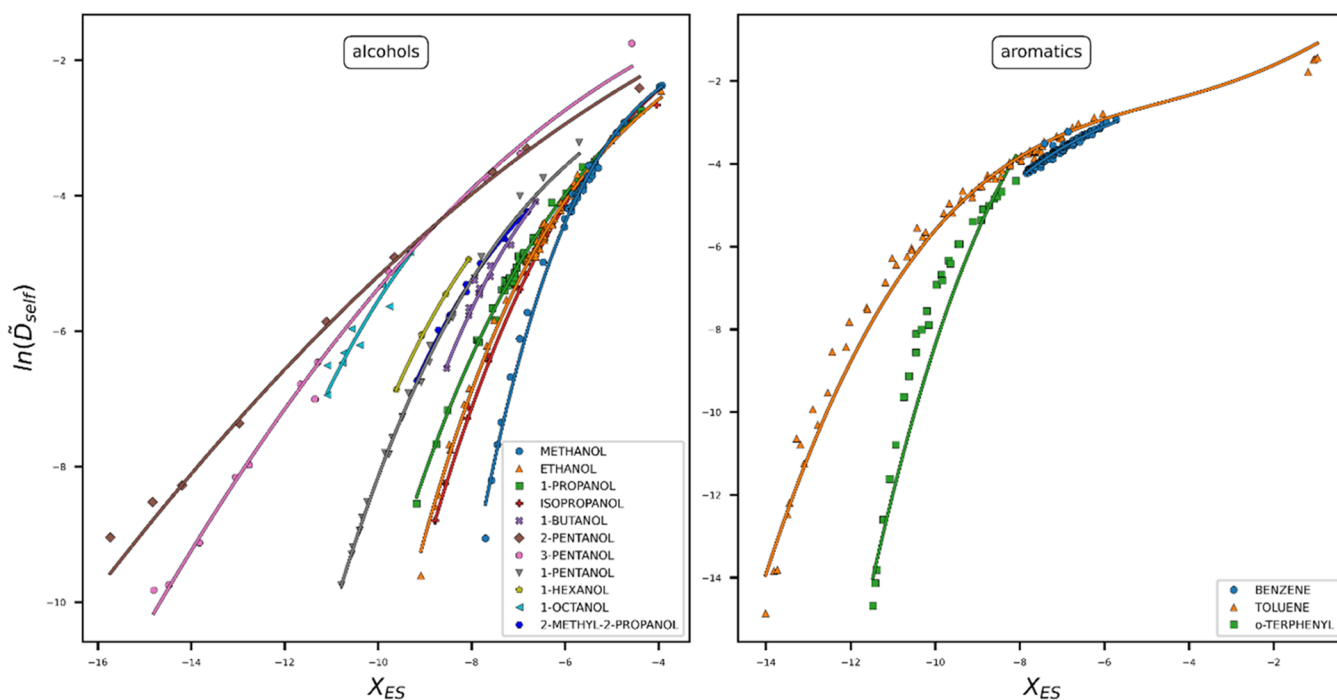
tc-PR - component-specific parameters

Figure 19. Application of the ES-based model combining eq 4 and parametrization strategy 1 to *n*-alcohols and aromatic compounds using the *tc*-PR EoS. Points: experimental data; solid line: model.

be safely used with EoSs that do not explicitly take the association into account.

It is noticeable that the deviations for aromatics are the largest (around 14%). This result was unexpected but a careful analysis of the data provided an explanation. First of all, among the three

molecules available in this family, benzene is very accurately correlated. The experimental data for toluene are very scattered, explaining why the average deviation for such a compound is above 20%. *o*-Terphenyl is poorly correlated. There is no theoretical explanation for such a behavior so that we are

tempted to believe that the data are questionable (a unique author made the measurements).

In the dense fluid region, self-associating and polar substances depart strongly from universal behavior, as attested by the comparison between Figures 14–17 (quasi-universal behavior) and Figures 18 and 19 (nonuniversal behavior). A loss of accuracy is observed, nonetheless, in very dense fluid conditions (near the solid-state region), where the self-diffusion phenomenon tends to cancel out. This is apparent for toluene (Figure 19) for which the magnitude of the available D_{self} experimental data ranges from 10^{-6} to 10^{-15} m²/s. The addition of a fourth parameter (a_4) in eq 4 (and more specifically, in the dense fluid part of this equation) would be necessary to model this extreme behavior. However, in the absence of a more comprehensive database, and because three a_i parameters were sufficient to represent most of the studied substances in the dense state, the a_4 parameter was not introduced.

Parametrization Strategy 2: Use of Chemical-Family-Specific Parameters. To overcome the potential lack of experimental data for a given compound, a second parametrization strategy for the proposed model equation (eq 4), involving chemical-family-specific parameters instead of component-specific parameters, is proposed. These parameters can be estimated, provided a sufficient number of representative compounds and data are available. For this reason, only four chemical families were eventually defined: *n*-alkanes, branched alkanes, cycloalkanes, and permanent gases. Parameters related to a given chemical family were fitted against all of the experimental data available for all of the components of the chemical family. Therefore, sets of parameters a_1 , a_2 , a_3 , b , c , and d in eq 4 were determined for each of the four chemical families defined above and are provided in the Supporting information. As was made for parametrization strategy 1, parameters b , c , and d were set to b_{univ} , c_{univ} , and d_{univ} , respectively, when fewer than three experimental data points were available in the dilute gas region ($X_{\text{ES}} \geq 0$).

As expected, chemical-family-specific parameters entailed a less accurate estimation of self-diffusion coefficients than component-specific ones, especially for large negative values of the Tv-residual entropy (i.e., at high densities) and for the branched alkane family. This effect is clearly visible by comparing Figures 5 and 20. To counterbalance the decrease in accuracy when switching from parametrization strategy 1 to 2, the second strategy makes it possible to predict self-diffusion coefficients for new molecules, provided that these molecules belong to one of the aforementioned chemical families. Eventually, chemical-family-specific parameters provide a reasonable alternative to parametrization strategy 1 when this latter cannot be used. The overall statistical results for parametrization strategy 2 (PS2) are shown in Figure 20. Similar deviations are obtained with *I*-PC-SAFT- and *tc*-PR-based models (MAPE = 9.5% in both cases).

The component-specific parametrization enables the description of the self-diffusion coefficient with an average accuracy of 7.5%, while when using a chemical-family parametrization, the deviation reaches 9.5%. These values are similar to those obtained by Hopp and Gross¹⁹ who reported an error of 8.2%. However, the model of Hopp and Gross¹⁹ inquires into the preliminary knowledge of a characteristic collision diameter, a characteristic energy of attraction between identical molecules and collision integrals. However, the accuracy of the proposed model is higher than that of the model recently developed by Zmpitas and Gross,³¹ who reported an average error of 12.3%.

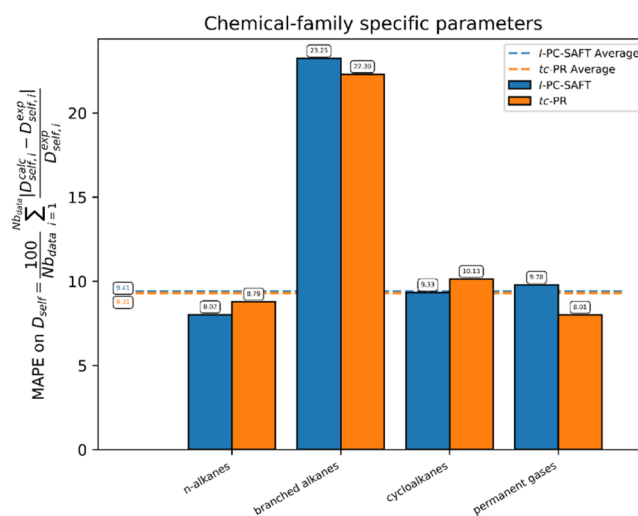


Figure 20. Prediction of self-diffusion coefficients using the model given by eq 4 and parametrization strategy 2 (with chemical-family-specific parameters). Summary of the MAPEs obtained using either the *I*-PC-SAFT or the *tc*-PR EoS for estimating density and residual entropy.

The performance of the model combining eq 4 and PS2 is illustrated in Figures 21–24.

To summarize this section, although the deviations obtained with PS2 are greater than those obtained with PS1, PS2 extends the prediction capacity of the ES concept. PS2 affords a reasonable estimation and a consistent description of the temperature and pressure dependence of the self-diffusion coefficient (Figures 21–24).

We observed that it was not possible to properly model the strong component dependence of the curves in dense states for some chemical families including associating compounds (e.g., alcohols) using PS2. For this reason, these chemical families were not modeled with this parameterization strategy.

Similar to the case where the parameters are component-specific (PS1) and for which we observed that the cubic and SAFT models were equivalent, the same conclusion can be drawn when PS2 is used: the *I*-PC-SAFT EoS and the *tc*-PR EoS give equivalent performances.

CONCLUSIONS

The present study was devoted to the development of a new model for the correlation of self-diffusion coefficients based on the entropy scaling concept. The main advantage of this approach lies in the applicability of the concept to the prediction of transport properties in any fluid state, from dense liquid to supercritical gas.

In this article, following a methodology developed for the correlation of shear viscosity in a previous article,¹⁵ a model relating a dimensionless form of the self-diffusion coefficient involving temperature and density [$Y_{\text{ES}} = \ln(\bar{D}_{\text{self}})$] and a function X_{ES} of the Tv-residual entropy were proposed.

As shown in Figure 3C, this model defines a unique mathematical relationship between Y_{ES} and X_{ES} for a given pure component, regardless of the state of the fluid (liquid, gas, or supercritical). In addition, a universal behavior at low density (i.e., for $X_{\text{ES}} > 0$) is highlighted.

To estimate the thermodynamic properties involved in the definition of X_{ES} and Y_{ES} (density and residual entropy), two

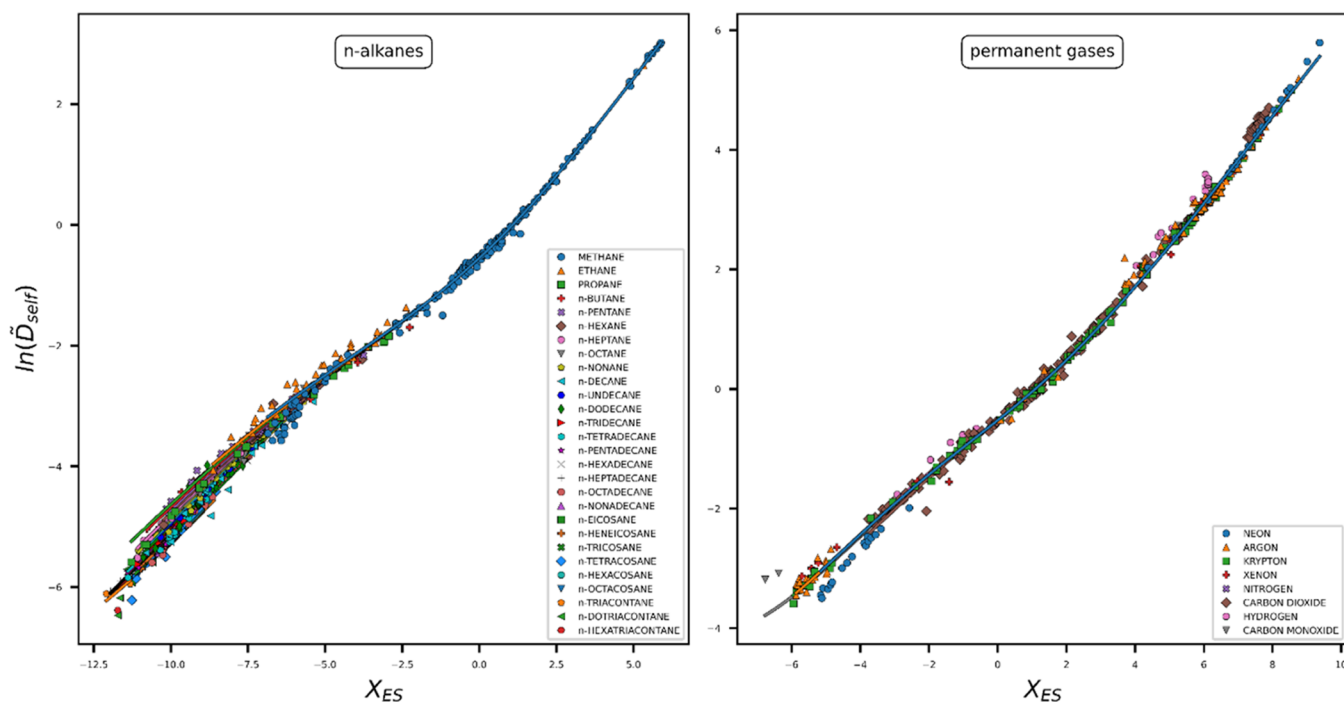
I-PC-SAFT - chemical-family specific parameters

Figure 21. Application of the ES-based model combining eq 4 and parametrization strategy 2 to *n*-alkanes and permanent gases using the *I*-PC-SAFT EoS. Points: experimental data; solid line: model.

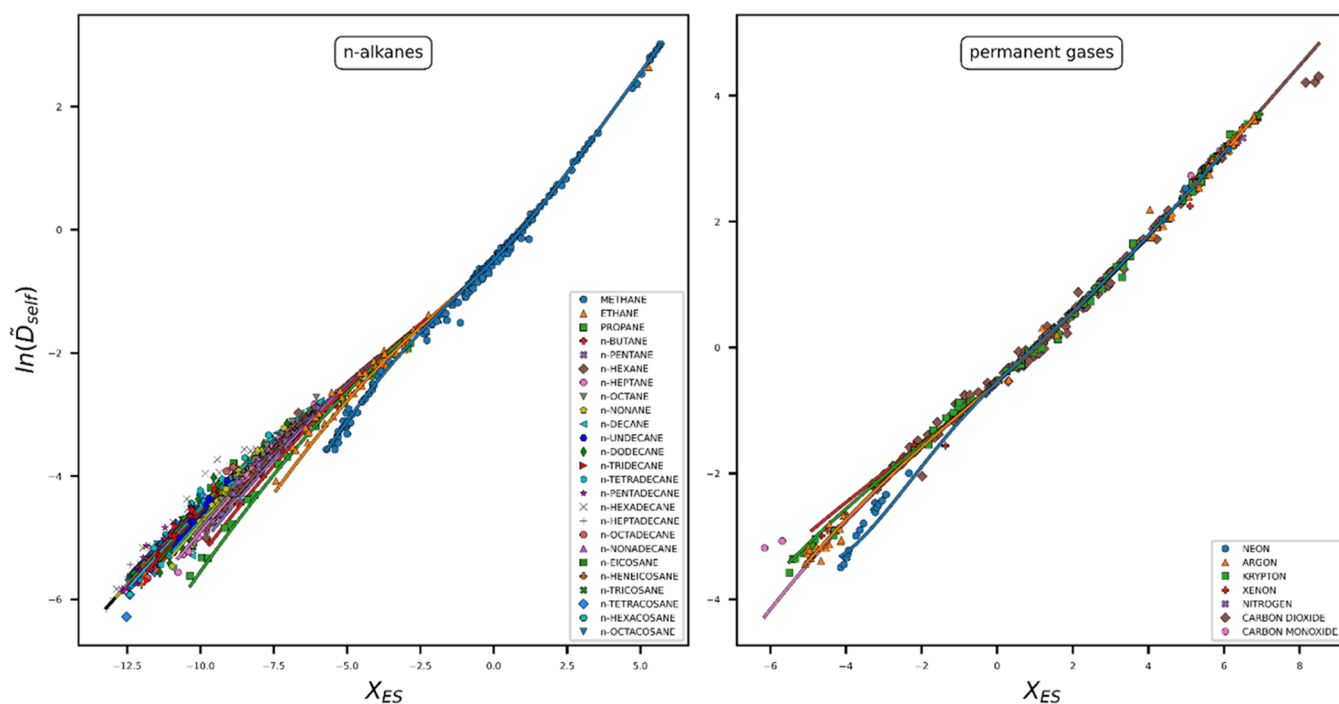
tc-PR - chemical-family specific parameters

Figure 22. Application of the ES-based model combining eq 4 and parametrization strategy 2 to *n*-alkanes and permanent gases using the *tc*-PR EoS. Points: experimental data; solid line: model.

EoS were selected: a SAFT-like EoS (*I*-PC-SAFT) and a cubic EoS (*tc*-PR).

Using a database containing ~ 2400 data for 72 pure species, two parametrization sets were determined for each EoS

- a component-specific set (i.e., for each component, model parameters were fit to data associated with this pure component),
- a chemical-family set (i.e., four chemical families were considered; for each of them, model parameters were

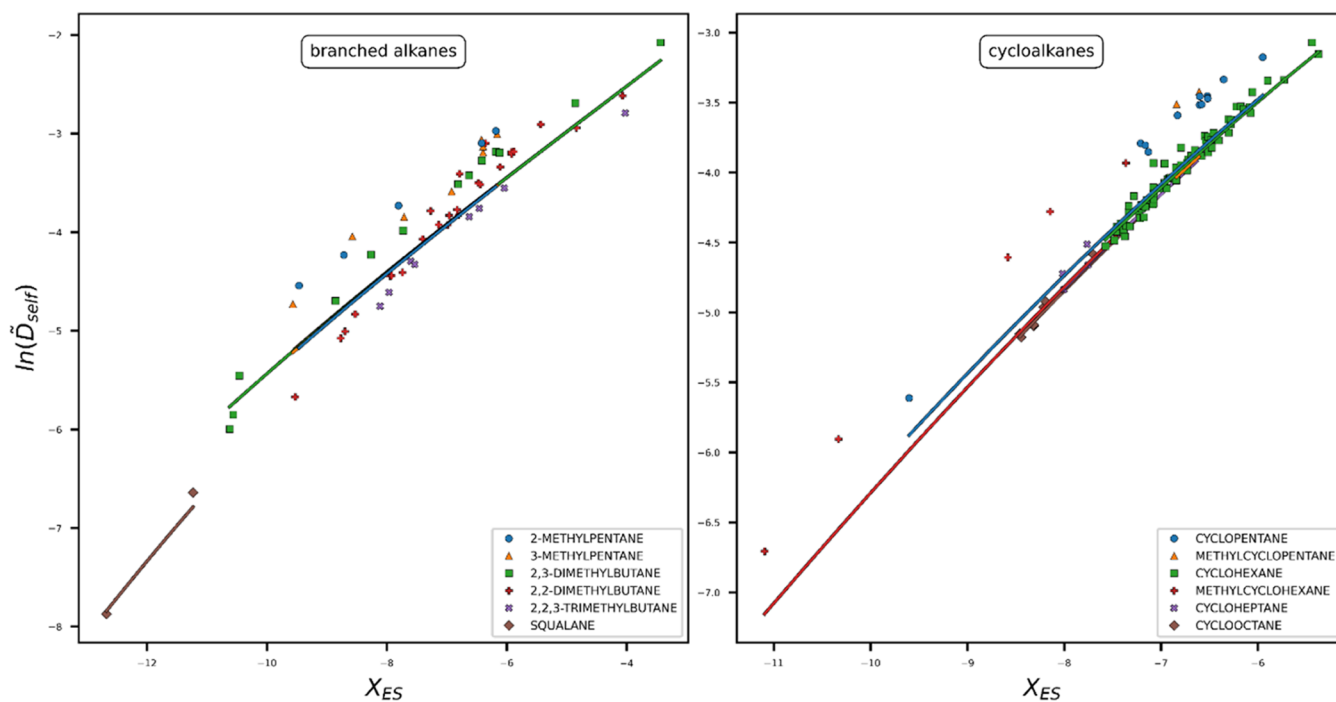
I-PC-SAFT - chemical-family specific parameters

Figure 23. Application of the ES-based model combining eq 4 and parametrization strategy 2 to aromatic compounds and ketones using the *I*-PC-SAFT EoS. Points: experimental data; solid line: model.

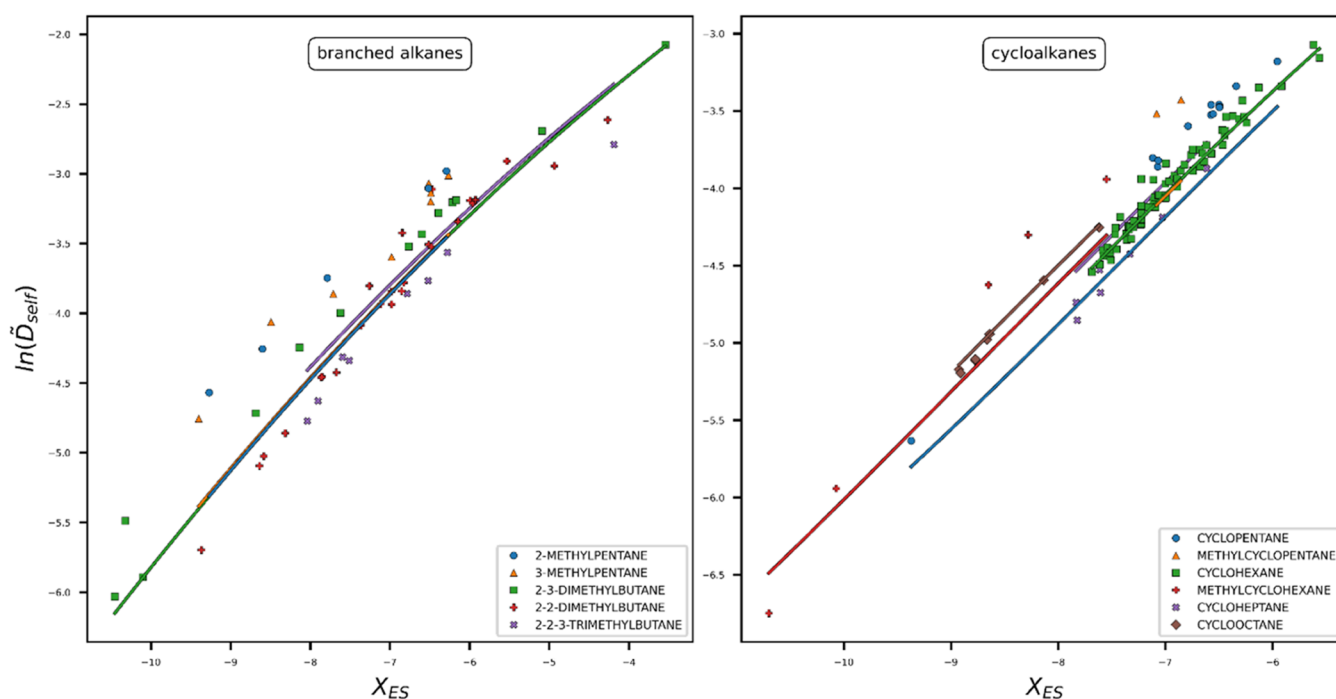
tc-PR - chemical-family specific parameters

Figure 24. Application of the ES-based model combining eq 4 and parametrization strategy 2 to aromatic compounds and ketones using the *tc*-PR EoS. Points: experimental data; solid line: model.

determined on data associated with all components belonging to the chemical family of interest).

Using a component-specific parametrization method, both EoSs lead to similar mean absolute deviations of $\sim 7.5\%$; while

using a chemical-family parametrization method, the deviation

for both EoSs is $\sim 9.5\%$.

■ ASSOCIATED CONTENT

SI Supporting Information

The Supporting Information is available free of charge at <https://pubs.acs.org/doi/10.1021/acs.iecr.2c01086>.

Presentation of the experimental database used for the ES-based correlation development; Parameters used with the I-PC-SAFT-based model; Parameters used with the *tc*-PR-based model (PDF)

Deviations between calculated and experimental self-diffusion coefficients for the 2400 experimental data points in the database used in this study (Excel file named: Database_component-specific_parameters_SAFT_CU-BIC.xlsx) (XLSX)

■ AUTHOR INFORMATION

Corresponding Authors

Jean-Noël Jaubert – Université de Lorraine, École Nationale Supérieure des Industries Chimiques, Laboratoire Réactions et Génie des Procédés (UMR CNRS 7274), 54000 Nancy, France; orcid.org/0000-0001-7831-5684; Email: jean-noel.jaubert@univ-lorraine.fr

Romain Privat – Université de Lorraine, École Nationale Supérieure des Industries Chimiques, Laboratoire Réactions et Génie des Procédés (UMR CNRS 7274), 54000 Nancy, France; orcid.org/0000-0001-6174-9160; Email: romain.privat@univ-lorraine.fr

Authors

Aghilas Dehlouz – Université de Lorraine, École Nationale Supérieure des Industries Chimiques, Laboratoire Réactions et Génie des Procédés (UMR CNRS 7274), 54000 Nancy, France; *Gaztransport & Technigaz (GTT)*, 78470 Saint-Rémy-lès-Chevreuse, France

Guillaume Galliero – Université de Pau et des Pays de l'Adour, E2S UPPA, CNRS TotalEnergies, LFCR UMR 5150, 64013 Pau, France; orcid.org/0000-0001-6393-8387

Marc Bonnissel – *Gaztransport & Technigaz (GTT)*, 78470 Saint-Rémy-lès-Chevreuse, France

Complete contact information is available at: <https://pubs.acs.org/doi/10.1021/acs.iecr.2c01086>

Notes

The authors declare no competing financial interest.

■ REFERENCES

- (1) Collell, J.; Galliero, G.; Vermorel, R.; Ungerer, P.; Yiannourakou, M.; Montel, F.; Pujol, M. Transport of Multicomponent Hydrocarbon Mixtures in Shale Organic Matter by Molecular Simulations. *J. Phys. Chem. C* **2015**, *119*, 22587–22595.
- (2) Tian, Y.; Xu, X.; Wu, J. Thermodynamic Route to Efficient Prediction of Gas Diffusivity in Nanoporous Materials. *Langmuir* **2017**, *33*, 11797–11803.
- (3) Tian, Y.; Fei, W.; Wu, J. Separation of Carbon Isotopes in Methane with Nanoporous Materials. *Ind. Eng. Chem. Res.* **2018**, *57*, 5151–5160.
- (4) Dahanayake, J. N.; Mitchell-Koch, K. R. Entropy Connects Water Structure and Dynamics in Protein Hydration Layer. *Phys. Chem. Chem. Phys.* **2018**, *20*, 14765–14777.
- (5) *Electrochemical Aspects of Ionic Liquids*, 2nd; Ohno, H., Ed.; Wiley: Hoboken, NJ, 2011.
- (6) Katsumata, R.; Dulaney, A. R.; Kim, C. B.; Ellison, C. J. Glass Transition and Self-Diffusion of Unentangled Polymer Melts Nanoconfined by Different Interfaces. *Macromolecules* **2018**, *51*, 7509–7517.
- (7) Guo, C. J.; de Kee, D. Effect of Molecular Size and Free Volume on Diffusion in Liquids. *Chem. Eng. Sci.* **1991**, *46*, 2133–2141.
- (8) Hirschfelder, J. O.; Curtiss, C. F.; Bird, R. B. *Molecular Theory of Gases and Liquids*, Corr. print. with notes added.; Structure of matter series; Wiley: New York, NY, 1964.
- (9) Reis, R. A.; Nobrega, R.; Oliveira, J. V.; Tavares, F. W. Self- and Mutual Diffusion Coefficient Equation for Pure Fluids, Liquid Mixtures and Polymeric Solutions. *Chem. Eng. Sci.* **2005**, *60*, 4581–4592.
- (10) Ricci, F. P.; Ricci, M. A.; Rocca, D. The Free Volume Theory and the Macedo-Litovitz Hybrid Equation for Diffusion in Liquids. *J. Phys. Chem. A* **1977**, *81*, 171–177.
- (11) Wanner, P.; Hunkeler, D. Isotope Fractionation Due to Aqueous Phase Diffusion – What Do Diffusion Models and Experiments Tell? – A Review. *Chemosphere* **2019**, *219*, 1032–1043.
- (12) Hoang, H.; Ho, K. H.; Battani, A.; Pujol, M.; Galliero, G. On Elemental and Isotopic Fractionation of Noble Gases in Geological Fluids by Molecular Diffusion. *Geochim. Cosmochim. Acta* **2021**, *315*, 172–184.
- (13) Suárez-Iglesias, O.; Medina, I.; de los Ángeles Sanz, M.; Pizarro, C.; Bueno, J. L. Self-Diffusion in Molecular Fluids and Noble Gases: Available Data. *J. Chem. Eng. Data* **2015**, *60*, 2757–2817.
- (14) Rosenfeld, Y. Relation between the Transport Coefficients and the Internal Entropy of Simple Systems. *Phys. Rev. A* **1977**, *15*, 2545–2549.
- (15) Dehlouz, A.; Privat, R.; Galliero, G.; Bonnissel, M.; Jaubert, J.-N. Revisiting the Entropy-Scaling Concept for Shear-Viscosity Estimation from Cubic and SAFT Equations of State: Application to Pure Fluids in Gas, Liquid and Supercritical States. *Ind. Eng. Chem. Res.* **2021**, *60*, 12719–12739.
- (16) Rosenfeld, Y. A Quasi-Universal Scaling Law for Atomic Transport in Simple Fluids. *J. Phys.: Condens. Matter* **1999**, *11*, 5415–5427.
- (17) Bell, I. H. Entropy Scaling of Viscosity—I: A Case Study of Propane. *J. Chem. Eng. Data* **2020**, *65*, 3203–3215.
- (18) Bell, I. H. Entropy Scaling of Viscosity—II: Predictive Scheme for Normal Alkanes. *J. Chem. Eng. Data* **2020**, *65*, S606–S616.
- (19) Hopp, M.; Mele, J.; Gross, J. Self-Diffusion Coefficients from Entropy Scaling Using the PC-SAFT Equation of State. *Ind. Eng. Chem. Res.* **2018**, *57*, 12942–12950.
- (20) Hopp, M.; Mele, J.; Hellmann, R.; Gross, J. Thermal Conductivity via Entropy Scaling: An Approach That Captures the Effect of Intramolecular Degrees of Freedom. *Ind. Eng. Chem. Res.* **2019**, *58*, 18432–18438.
- (21) Lötgering-Lin, O.; Gross, J. Group Contribution Method for Viscosities Based on Entropy Scaling Using the Perturbed-Chain Polar Statistical Associating Fluid Theory. *Ind. Eng. Chem. Res.* **2015**, *54*, 7942–7952.
- (22) Lötgering-Lin, O.; Fischer, M.; Hopp, M.; Gross, J. Pure Substance and Mixture Viscosities Based on Entropy Scaling and an Analytic Equation of State. *Ind. Eng. Chem. Res.* **2018**, *57*, 4095–4114.
- (23) Fouad, W. A.; Alasiri, H. Molecular Dynamic Simulation and SAFT Modeling of the Viscosity and Self-Diffusion Coefficient of Low Global Warming Potential Refrigerants. *J. Mol. Liq.* **2020**, *317*, No. 113998.
- (24) Eller, J.; Sauerborn, T.; Becker, B.; Buntic, I.; Gross, J.; Helmig, R. Modeling Subsurface Hydrogen Storage with Transport Properties from Entropy Scaling Using the PC-SAFT Equation of State. *Water Resour. Res.* **2022**, *58*, No. e2021WR030885.
- (25) Dzугutov, M. A Universal Scaling Law for Atomic Diffusion in Condensed Matter. *Nature* **1996**, *381*, 137–139.
- (26) Chapman, S.; Cowling, T. G. *The Mathematical Theory of Non-Uniform Gases: An Account of the Kinetic Theory of Viscosity, Thermal Conduction, and Diffusion in Gases*, 3rd ed.; Cambridge mathematical library; Cambridge University Press: Cambridge; New York, 1990.
- (27) Bretonnet, J.-L. Self-Diffusion Coefficient of Dense Fluids from the Pair Correlation Function. *J. Chem. Phys.* **2002**, *117*, 9370–9373.
- (28) Krekelberg, W. P.; Pond, M. J.; Goel, G.; Shen, V. K.; Errington, J. R.; Truskett, T. M. Generalized Rosenfeld Scalings for Tracer Diffusivities in Not-so-Simple Fluids: Mixtures and Soft Particles. *Phys. Rev. E* **2009**, *80*, No. 061205.

- (29) Novak, L. Self-Diffusion Coefficient and Viscosity in Fluids. *Int. J. Chem. React. Eng.* **2011**, *9*, No. e2021WR030885.
- (30) Novak, L. T. Predictive Corresponding-States Viscosity Model for the Entire Fluid Region: *N*-Alkanes. *Ind. Eng. Chem. Res.* **2013**, *52*, 6841–6847.
- (31) Zmpitas, J.; Gross, J. Modified Stokes–Einstein Equation for Molecular Self-Diffusion Based on Entropy Scaling. *Ind. Eng. Chem. Res.* **2021**, *60*, 4453–4459.
- (32) Dyre, J. C. Perspective: Excess-Entropy Scaling. *J. Chem. Phys.* **2018**, *149*, No. 210901.
- (33) Bell, I. H.; Messerly, R.; Thol, M.; Costigliola, L.; Dyre, J. C. Modified Entropy Scaling of the Transport Properties of the Lennard-Jones Fluid. *J. Phys. Chem. B* **2019**, *123*, 6345–6363.
- (34) Dehlouz, A.; Jaubert, J.-N.; Galliero, G.; Bonnissel, M.; Privat, R. Combining the Entropy-Scaling Concept and Cubic- or SAFT Equations of State for Modelling Thermal Conductivities of Pure Fluids. *Int. J. Heat Mass Transfer* **2022**, DOI: 10.1016/j.ijheatmasstransfer.2022.123286.
- (35) Moine, E.; Piña-Martinez, A.; Jaubert, J.-N.; Sirjean, B.; Privat, R. I-PC-SAFT: An Industrialized Version of the Volume-Translated PC-SAFT Equation of State for Pure Components, Resulting from Experience Acquired All through the Years on the Parameterization of SAFT-Type and Cubic Models. *Ind. Eng. Chem. Res.* **2019**, *58*, 20815–20827.
- (36) Jaubert, J.-N.; Privat, R.; Le Guennec, Y.; Coniglio, L. Note on the Properties Altered by Application of a Peneloux-Type Volume Translation to an Equation of State. *Fluid Phase Equilib.* **2016**, *419*, 88–95.
- (37) Privat, R.; Jaubert, J.-N.; Le Guennec, Y. Incorporation of a Volume Translation in an Equation of State for Fluid Mixtures: Which Combining Rule? Which Effect on Properties of Mixing? *Fluid Phase Equilib.* **2016**, *427*, 414–420.
- (38) Le Guennec, Y.; Lasala, S.; Privat, R.; Jaubert, J.-N. A Consistency Test for α -Functions of Cubic Equations of State. *Fluid Phase Equilib.* **2016**, *427*, 513–538.
- (39) Le Guennec, Y.; Privat, R.; Lasala, S.; Jaubert, J.-N. On the Imperative Need to Use a Consistent α -Function for the Prediction of Pure-Compound Supercritical Properties with a Cubic Equation of State. *Fluid Phase Equilib.* **2017**, *445*, 45–53.
- (40) Le Guennec, Y.; Privat, R.; Jaubert, J.-N. Development of the Translated-Consistent *tc*-PR and *tc*-RK Cubic Equations of State for a Safe and Accurate Prediction of Volumetric, Energetic and Saturation Properties of Pure Compounds in the Sub- and Super-Critical Domains. *Fluid Phase Equilib.* **2016**, *429*, 301–312.
- (41) Piña-Martinez, A.; Privat, R.; Jaubert, J. Use of 300,000 Pseudo-experimental Data over 1800 Pure Fluids to Assess the Performance of Four Cubic Equations of State: SRK, PR, *tc*-RK, and *tc*-PR. *AIChE J.* **2022**, *68*, No. e17518.
- (42) Ramírez-Vélez, N.; Privat, R.; Pina-Martinez, A.; Jaubert, J. Assessing the Performance of Non-associating SAFT-type Equations of State to Reproduce Vapor Pressure, Liquid Density, Enthalpy of Vaporization, and Liquid Heat Capacity Data of 1800 Pure Fluids. *AIChE J.* **2022**, *68*, No. e17722.
- (43) Santos, J. R. C.; Abreu, P. E.; Marques, J. M. C. Calculation of Diffusion Coefficients of Pesticides by Employing Molecular Dynamics Simulations. *J. Mol. Liq.* **2021**, *340*, No. 117106.
- (44) Fischer, M.; Bauer, G.; Gross, J. Transferable Anisotropic United-Atom Mie (TAMIE) Force Field: Transport Properties from Equilibrium Molecular Dynamic Simulations. *Ind. Eng. Chem. Res.* **2020**, *59*, 8855–8869.
- (45) Zhang, L.; Liu, C.; Liu, Y.; Li, Q.; Cheng, Q.; Cai, S. Transport Property of Methane and Ethane in K-illite Nanopores of Shale: Insights from Molecular Dynamic Simulations. *Energy Fuels* **2020**, *34*, 1710–1719.
- (46) Moulτος, O. A.; Zhang, Y.; Tsimpanogiannis, I. N.; Economou, I. G.; Maginn, E. J. System-Size Corrections for Self-Diffusion Coefficients Calculated from Molecular Dynamics Simulations: The Case of CO₂, *n*-Alkanes, and Poly(Ethylene Glycol) Dimethyl Ethers. *J. Chem. Phys.* **2016**, *145*, No. 074109.

Recommended by ACS

Generalized Form for Finite-Size Corrections in Mutual Diffusion Coefficients of Multicomponent Mixtures Obtained from Equilibrium Molecular Dynamics Simulation

Seyed Hossein Jamali, Othonas A. Moulτος, *et al.*

APRIL 27, 2020

JOURNAL OF CHEMICAL THEORY AND COMPUTATION

READ 

Fick Diffusion Coefficient Matrix of a Quaternary Liquid Mixture by Molecular Dynamics

Gabriela Guevara-Carrion, Jadran Vrabec, *et al.*

MARCH 23, 2020

THE JOURNAL OF PHYSICAL CHEMISTRY B

READ 

Revisiting the Entropy-Scaling Concept for Shear-Viscosity Estimation from Cubic and SAFT Equations of State: Application to Pure Fluids in Gas, Liquid and Supercritical...

Aghilas Dehlouz, Jean-Noël Jaubert, *et al.*

AUGUST 18, 2021

INDUSTRIAL & ENGINEERING CHEMISTRY RESEARCH

READ 

Thermophysical Properties of the Lennard-Jones Fluid: Database and Data Assessment

Simon Stephan, Hans Hasse, *et al.*

OCTOBER 14, 2019

JOURNAL OF CHEMICAL INFORMATION AND MODELING

READ 

Get More Suggestions >